P-08-41

Oskarshamn site investigation

Mineralogy in water conducting zones

Results from boreholes KLX03, KLX04, KLX06, KSH01A+B, KSH02 and KSH03A

Henrik Drake, Isochron GeoConsulting HB
Eva-Lena Tullborg, Terralogica AB

July 2008

Svensk Kärnbränslehantering AB
Swedish Nuclear Fuel
and Waste Management Co

Box 250, SE-101 24 Stockholm
Phone +46 8 459 84 00

ISSN 1651-4416
SKB P-08-41

Oskarshamn site investigation

Mineralogy in water conducting zones

Results from boreholes KLX03, KLX04, KLX06, KSH01A+B, KSH02 and KSH03A

Henrik Drake, Isochron GeoConsulting HB
Eva-Lena Tullborg, Terralogica AB

July 2008

Keywords: Water conducting zones, Mineralogy, Chemistry, X-ray diffraction, SEM-EDS, Stable isotopes, U–series disequilibrium, Laxemar, Simpevarp.

Abstract

This report is part of the SKB site investigations in Oskarshamn. The report includes results from detailed studies of fracture coatings/fillings from water conducting sections in bore holes KLX03, KLX04 and KLX06 in the Laxemar subarea. Samples are preferably selected from sections sampled for complete chemical characterization. Additional samples from boreholes KSH01A+B, KSH02 and KSH03A in the Simpevarp subarea are also included. Methods used are mineral identification (XRD, SEM-EDS), chemistry (ICP-AES/QMS), and isotope ratios (USD, $\delta^{13}C$, $\delta^{18}O$). The results presented in this report constitute only a minor part of all the fracture mineral analyses carried out within the investigation program for the Oskarshamn site investigation subareas and constitutes no thorough interpretations.

Sammanfattning

Denna rapport ingår i SKB:s platsundersökningar i Oskarshamn. I rapporten presenteras resultat från detaljerade undersökningar av sprickfyllningar/beläggningar i vattenförande zoner i borrhål KLX03, KLX04 och KLX06 i delområde Laxemar (speciellt sektioner provtagna för fullständig kemikaraktärisering). Ytterligare prover från borrhål KSH01A+B, KSH02 och KSH03A från delområde Simpevarp är också inkluderade i denna rapport. Metoder som använts är mineral-identifikation (SEM-EDS, XRD), kemi (ICP-AES/QMS), och isotopkvoter (USD, $\delta^{13}C$, $\delta^{18}O$). De resultat som presenteras här utgör endast en bråkdel av de sprickmineralogiska analyser som utförts inom alla delområden i Oskarshamns platsundersökningsområde och inga omfattande tolkningar av data redovisas därför i denna rapport.

Contents

1 Introduction

This report is part of the SKB site investigations in Oskarshamn. The report includes results from detailed studies of fracture coatings/fillings from water conducting sections in bore holes KLX03, KLX04 and KLX06 (Figure 1-1) in the Laxemar subarea /Ask et al. 2005ab/. Samples are preferably selected from sections sampled for complete chemical characterization. Additional samples from boreholes KSH01A+B, KSH02 and KSH03A in the Simpevarp subarea are also included. See /Drake and Tullborg 2004/ (for detailed sample descriptions, XRD results, $\delta^{13}C$, and $\delta^{18}O$). In Table 1-1 controlling documents for performing this activity are listed. Both activity plans and method descriptions are SKB's internal controlling documents. Results from the present study of boreholes KLX03, KLX04, KLX06, KSH01A+B, KSH02 and KSH03A, have been compared to results from other studies in the subareas of Laxemar, Äspö, and Simpevarp /e.g. Wallin and Peterman 1999, Bath et al. 2000, Drake and Tullborg 2004, 2006a, Milodowski et al. 2005/.

Included in the detailed studies of the water conducting sections are mineral identification (XRD, SEM-EDS), mineral chemistry (SEM-EDS, ICP-AES/QMS), stable isotopes ($\delta^{13}C$, $\delta^{18}O$ in calcite) and U-series analyses.

Table 1-1. Controlling documents for the performance of the activity

Activity plan	**Number**	**Version**
Sprickmineralogiska undersökningar i KLX03, KLX04 och KLX06	AP-PS-400-05-053	1.0
Sprickmineralogiska undersökningar i KSH02 och KSH03	AP-PS-400-05-052	1.0
Sprickmineralogiska undersökningar i KSH01	AP-PS-400-03-045	1.0
Method descriptions	**Number**	**Version**
Sprickmineralanalys	SKB MD 144.001	1.0

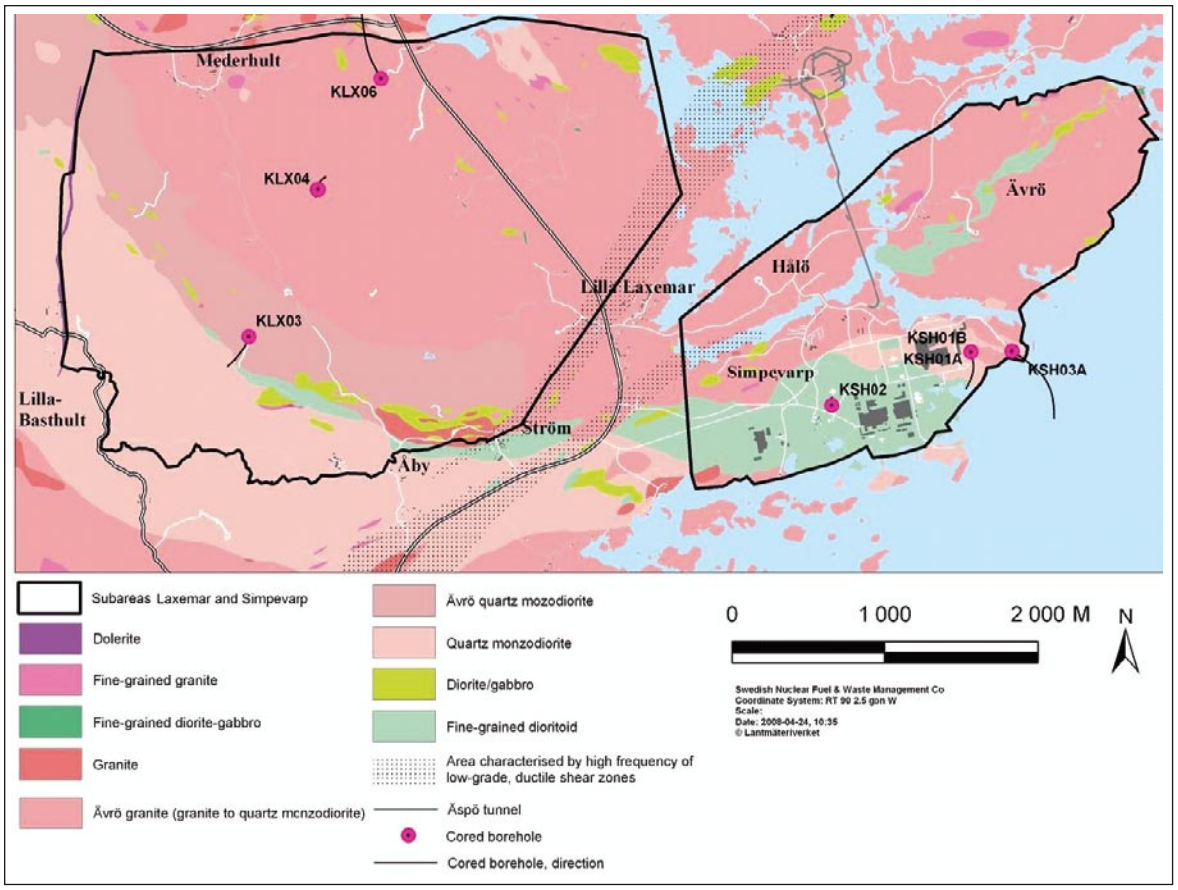

Figure 1-1. *Geological map of the Oskarshamn site investigation area with the investigated boreholes KLX03, KLX04, KLX06, KSH01A+B, KSH02 and KSH03A shown.*

2 Objective and scope

The objective and scope have been to investigate the mineralogy (SEM-EDS and XRD), chemistry (ICP-AES/QMS) and isotope characteristics ($\delta^{13}C$, $\delta^{18}O$ and U-series) of sections sampled for complete chemical characterisation in bore holes KLX03 and KLX04 /Ask et al. 2005ab/, Laxemar subarea. Additional samples from bore hole KLX06, Laxemar subarea (not in sections sampled for chemical characterization) are also included together with samples from KSH01A+B, KSH02 and one sample from KSH03A, all three in Simpevarp subarea. The task has been to:

- Identify minerals; the drill core mapping is based on macroscopic determination of fracture minerals. SEM-analysis or XRD is needed to give a more detailed and precise description of the mineralogy in water conducting sections.
- Give input to hydrogeochemical modelling and give a background to paleohydrogeological interpretations.

3 Equipment

3.1 Description of equipment

The following equipment was used in the investigations:

- Scanning electron microscope (Hitachi S-3400N) with EDS (Oxford Instruments).
- Stereo microscope (Leica MZ12).
- Digital camera (Konica Revio KD-420Z).
- Rock saw.
- Rock Labs swing mill.
- Knife.
- Magnifying lens – 10x.
- Scanner (Epson 3200).
- Computer software, e.g. Corel Draw 11, Microsoft Word, Microsoft Excel, Link ISIS.
- Mass-spectrometer.

All equipment listed above is property of Earth Sciences Centre, University of Gothenburg, or the authors. For equipment used for whole rock chemistry analyses, U-series analyses, X-ray diffraction and stable isotope analyses, see chapter 4 below.

4 Execution

4.1 Sample collection and preparations

The sampling was focused on sections sampled for complete chemical characterization in KLX03 and from transmissive fractures in KLX04 and KLX06 /Ask et al. 2005ab/. Unfortunately, some of these sections did not include suitable samples. Therefore, samples were also collected in the possibly less water conducting zones, scattered throughout the drill core (however, mostly focused on water conducting zones of low transmissivity). Flow logs were used as a support to the sampling /Rouhiainen and Sokolnicki 2005, Rouhiainen et al. 2005, Sokolnicki and Rouhiainen 2005/. Additional samples from boreholes KSH01A+B, KSH02 and KSH03A in the Simpevarp subarea were also chosen to represent transmissive fractures.

The fracture surface of most of the samples was removed (by sawing if needed), glued to a glass plate to obtain a horizontal surface and scanned in order to support the SEM investigations. SEM-EDS was used to identify the major minerals (as well as some minor and accessory), and to characterize the fracture surface morphology.

After this procedure, the minerals on the fracture surfaces of the samples were scraped off using a knife. This material was then sieved and the grains smaller than 0.125 mm were collected for U-series analysis. The rest of the material was milled to a grain size smaller than 0.125 mm. The major part of the milled material was then added to the material collected for U-series analyses and the remaining material was collected for ICP-AES and ICP-QMS chemical analyses and X-ray diffraction (if enough material was obtained).

Samples including a significant amount of calcite were investigated with a hand lens, stereo microscope and SEM in order to identify the crystal morphology, if possible. The calcite crystals were then scraped off with a knife. This material was checked for purity in stereo microscope and then analysed for stable isotopes $\delta^{18}O$ and $\delta^{13}C$.

Investigation methods for each sample are listed in Table 4-1.

Table 4-1. Investigation methods for all the samples.

Section* (m)	Sample (m)	ICP-AES/ ICP-QMS	XRD	U-series	$\delta^{13}C/\delta^{18}O$**	SEM
KLX03						
	129.37–129.37				X	
	130.60–130.61				X	
	165.52–165.55				X	
	168.47–168.54		X	X		
193.5–198.3*	195.36–195.36	X	X	X		X
	204.30–204–36				XX	
	276.71–276.81				XX	
	288.72–288.76				X	
	303.21–303.21				X	
	305.80–305.99				X	
	326.94–327.04		X	X		X
	327.40–327.62				X	
	353.54–353.62				X	
	397.79–397.89		X	X		X
408–415*	409.83–410.13		X	X	XX	X
	457.33–457.42				X	

	534.25–534.40	X		X		
	590.79–590.96				X	
660–671*	662.33–662.65		X		XX	X
735.5–748.03*	743.98–744.06		X	X		X
	771.95–772.06				X	
	772.24–772.27				X	
	784.71–784.79				X	
	904.38–904.54		X	X		X
	904.90–905.06				X	
964–975*	969.21–969.27					X
KLX04						
103–213*	105.86–105.96				X	
103–213*	107.08–107.43				XX	
103–213*	139.08–139.13			X	X	
103–213*	193.74–193.90	X	X	X		X
103–213*	201.04–201.20				X	
	216.66–216.79		X	X		
	352.69–352.81		X	X	X	X
510–515*	513.53–513.70	X		X	X	
	555.27–555.44				X	
	580.70–580.82				X	
	626.51–626.58				X	
	643.18–643.40				X	
	917.40–917.51				XX	
971.21–976.21*	972.13–972.20				X	
KLX06						
	214.11–214.16	X	X	X		X
	383.93–383.93	X	X	X		X
	388.27–388.30	X	X	X		X
	3.70–3.87	X		X		
	8.6			X		
	8.70–8.75			X		
	67.8–67.9	X		X		
	82.20	X		X		
	159.2–159.3	X		X		
	250.40–250.45	X		X		
	255.78–255.93	X		X		
	558.60–558.65	X		X		
	590.36–590.52	X		X		
KSH02						
	104				XX	
	289.00–280.05	X	X	X	X	
	422.9				X	
	423				X	
	578.00–578.05	X	X	X		
	743.00–743.05	X	X	X	X	
KSH03A						
	272.00–272.50	X		X		

*=Sections sampled for complete ground water characterization
**=Calcite

4.2 SEM-EDS analyses

The SEM investigations and EDS micro analyses were carried out on an Oxford Instruments Energy Dispersive System mounted on a Hitachi S-3400N scanning electron microscope at the Earth Sciences Centre, University of Gothenburg, Sweden. The acceleration voltage was 20 kV, the working distance 10 mm and the specimen current was about 1nA. The investigations were carried out using low-vacuum mode (15–20 Pa). The instrument was calibrated at least twice every hour using a cobalt standard linked to simple oxide and mineral standards, to confirm that the drift was acceptable. X-ray spectrometric corrections were made by an on-line computer system. Proper mineral analyses were not carried out due to the uneven surface of the samples which causes too low total values (a polished surface is needed). The mineralogy (except for clay minerals) was identified based on element ratios and spectra of each element of the different minerals.

4.3 ICP-AES, ICP-QMS

ICP-AES/ICP-QMS analyses were carried out by Analytica AB. For most elements the following procedure was applied: 0.125 g sample is fused with 0.375 g $LiBO_2$ and dissolved in dilute HNO_3. For Co, Cu, Ni and Zn analyses however, digestion was done by microwave heating in closed teflon vessels with HNO_3/H_2O 1:1. LOI (Loss on ignition) is carried out at 1,000°C (some samples were too small to perform LOI). Concentrations of the elements are determined by ICP-AES and ICP-QMS. Analyses are carried out according to EPA methods (modified) 200.7 (ICP-AES) and 200.8 (ICP-QMS).

4.4 X-ray diffraction

The analyses were carried out by SGU, Uppsala, Sweden, according to the following procedure. Samples > 0.40 g were divided with a sample separator and of which one part was milled in an agate mortar. All the material from samples < 0.40 g was milled to a fine powder. The powder was packed in a small sampler for XRD-analysis and identification of major minerals. Extremely small samples were put on a silicon plate and suspended in alcohol to spread the material over the plate. The samples were then dried and XRD-analysis was performed.

The clay-rich samples were dispersed in distilled water, filtered and oriented according to /Drever 1973/. For samples of small volumes the suspension was repeatedly put on a glass plate and dried. Three measurements were carried out on each of the fine fraction samples for clay mineral identification; 1) dried samples, 2) saturated with ethyleneglycol for two hours, and finally 3) after heating to 400°C in two hours. Coarser material was wet sieved and dried. The > 35µm fraction was ground by hand in an agate mortar. The sample powder was randomly orientated in the sample holder (and very small sample volumes on a piece of glass). The radiation (CuK_α) in the diffractometer was generated at 40 kV and 40 mA, and the X-rays were focussed with a graphite monochromator. Scans were run from 2°–65° (2-theta) or from 2°–35° (samples with preferred crystal orientation) with step size 0.02° (2-theta) and counting time 1 s $step^{-1}$. The analyses were performed with a fixed 1° divergence and a 2 mm receiving slit. The XRD raw files were taken up in the Bruker/Siemens $DIFFRAC^{PLUS}$ software (version 2.2), and evaluated in the programme EVA. The minerals were identified by means of the /PDF 1994/ computer database.

4.5 U-series analyses

The Uranium-Thorium analyses were carried out at the Scottish Universities Environmental Research Centre, Scotland, accordingly: Sample material was furnaced at 600°C (in increments of 100°C if material is highly organic). The material was washed from the crucible with H_2O into a beaker, some 9M HCl was add as well as spike (spike was left to equilibrate to room temperature before adding and allow for equilibration within the sample). Digestions using Aqua regia ($1HCl:1HNO_3$), H_2O_2 and HF were carried out as required, taking to near dryness for each, except HF where complete dryness is required. Then leaching with 4M HNO_3 was carried out and an $Fe(OH)_3$ scavenge using NH_3 was then carried out. The precipitate formed was washed thoroughly and dissolved in a minimum concentration HCl and transferred to a clean beaker. The solution was dried down and taken up in ~50 ml 9M HCl and a DIPE (di-isopropylether) extraction was carried out to remove any Fe within the sample. The first (chloride) column was pre-conditioned with ~20 ml of 1.2M HCl and 9M HCl. The sample was introduced to the column in 9M HCl and the Th fraction collected by washing with (2x25 ml) 9M HCl. The U fraction was eluted with 150 ml 1.2M HCl. The U fraction was taken to dryness and prepared for electrodepositioning. The Th fraction was taken to dryness and taken back up in 4M HNO_3 (approximately 50 ml) and an aluminium precipitation carried out with NH_4OH. Precipitate formed was washed well and dissolved in the minimum concentration HNO_3. The solution was then dried down and taken back up in 8M HNO_3 (approximately 50 ml) ready for the second (nitric) column. Second column was pre-conditioned with ~20 ml 1.2M HCl and 8M HNO_3. The Th sample was introduced to the column in 8M HNO_3, and rinsed with 2 x 25 ml aliquots 8M HNO_3. The Th fraction was then eluted with 100 ml 9M HCl and then the Th fraction was taken to dryness and prepared for electrodepositioning. Th is electrodeposited from the NH_4Cl solution onto a stainless steel planchette for alpha spectroscopy analysis. The planchette is placed on a sample holder of an EG&G Ortec (AMETEC) Octete alpha spectroscopy system and the sample holder is moved close to the detector face. Detectors are of 450 mm^2 surface area, 20 μm depletion depth Si surface barrier detectors with resolution better than 20 keV. The Octete has 8 chambers, each containing a detector of this type. The detector chamber is evacuated using an oil free vacuum pump and alpha spectra are recorded until sufficient counts (aim was 5,000) are obtained in all of the peaks of interest. Peak area identification and analysis is done by visual inspection of spectra and use of the EG&G programme Maestro 2. Specific activities of the nuclides are calculated on the basis of the peak areas, the known spike activity and the sample weights.

4.6 $\delta^{13}C$ and $\delta^{18}O$

The stable carbon and oxygen isotope analyses carried out at the Earth Sciences Centre, University of Gothenburg, Sweden, on 36 calcite samples were made accordingly: Samples, usually between 150 and 250 μg each, were roasted in vacuum for 30 minutes at 400°C to remove possible organic material and moisture. Thereafter, the samples were analysed using a VG Prism Series II mass spectrometer with a VG Isocarb preparation system on line. In the preparation system each sample was reacted with 100% phosphoric acid at 90°C for 10 minutes, whereupon the released CO_2 gas was analysed in the mass spectrometer. All isotope results are reported as δ per mil relative to the Vienna Pee Dee Belemnite (VPDB) standard. The analysing system is calibrated to the PDB scale via NBS-19.

5 Results

5.1 Mineralogy

Most of the samples contained fractures that have been activated more then once. This is evidenced by old fracture sets (sometimes cataclasites) with a certain mineralogy (usually epidote, chlorite, quartz, calcite, prehnite, K-feldspar, hematite, illite etc.), which have been re-activated and sometimes cut by younger fractures. The mineralogy on the fracture surfaces of these relatively late open fractures are of certain interest for this report. Most of the sampled fractures contained clay minerals (often corrensite, mixed layer clay [smectite/illite] and illite), chlorite, hematite, pyrite, calcite and wall rock fragments such as K-feldspar, quartz, plagioclase and titanite, on their surfaces. REE-carbonate, barite, galena, fluorite, apophyllite, gypsum, U-rich silicates and later formed quartz and K-feldspar are found on the fracture surfaces on some of the samples. Sample descriptions and of samples from KLX03, KLX04 and KLX06, are found in Appendix 1 and for samples from KSH01A+B are found in /Drake and Tullborg 2004/. XRD analyses of samples from KLX03, KLX04 and KLX06 are found in Appendix 1, as well as in Appendix 2. XRD analyses of samples from KSH01A+B, KSH02 and KSH03A are found in Appendix 7. The mineralogy identified with SEM-EDS and XRD differs somewhat because XRD samples are scraped off from the surface (underlying material might be included), while only the uppermost layer on the fracture surfaces are investigated with SEM-EDS.

The fracture surface morphology varies widely between different samples and within a single sample. The most common feature is a fairly smooth surface with minor parts of the surface being more rugged due to crystal aggregates (commonly only visible using SEM). The crystals in the smooth parts are sometimes striated (especially chlorite and clay minerals but also calcite). The crystals grown on the striated surfaces are often euhedral, e.g. cubic pyrite and fluorite, and scalenohedral or equant calcite.

Most of the samples show altered, red-stained wall rock adjacent to the fractures. The characteristics of this red-staining have been studied in samples from drill cores KLX04, Laxemar subarea /Drake and Tullborg 2006b/ as well as from KSH01A+B and KSH03A+B, Simpevarp subarea /Drake and Tullborg 2006c/, respectively. The red-stained rock shows alteration of plagioclase, biotite and magnetite, formation of secondary albite, adularia, chlorite, prehnite and hematite as well as small changes in chemistry and reducing capacity compared to the fresh rock. This alteration has taken place during hydrothermal conditions.

5.2 Chemistry

Results from the chemical analyses from most samples are found in Appendix 2 (results from KSH01A+B, KSH02 and KSH03A are found in Appendix 5). The samples with a high amount of chlorite and clay minerals are enriched in e.g. Fe, Mg and Al compared to the host rock while samples with a high amount of calcite are enriched in Ca compared to the host rock. The Ba content is very high in two samples (9,720 ppm in KSH01A: 159.2–159.3 m and 15,400 ppm in sample KLX03:195.36–195.36 m) possibly due to the presence of barite and/or harmotome, although none of these minerals were identified with SEM-EDS or XRD. U and Th concentrations in the 19 samples analysed are 1–23 ppm and 0.25–20 ppm, respectively. 9 of the 19 samples analysed for whole rock chemistry have higher Cs concentrations than the wall rock (< 3 ppm Cs), especially the samples with mixed layer clay are high in Cs e.g. KLX06: 383.93–383.92 m where Cs amounts to 103 ppm. Chondrite-normalised REE-patterns are shown in Figure 5-1 (Laxemar subarea samples) and Figure 5-2 (Simpevarp subarea samples). The REE-patterns of the Laxemar subarea samples are very similar to the REE-patterns for the host rock (Ävrö granite) Figure 5-3. The Simpevarp subarea samples generally show similar, relatively flat REE pattern as the Laxemar subarea samples.

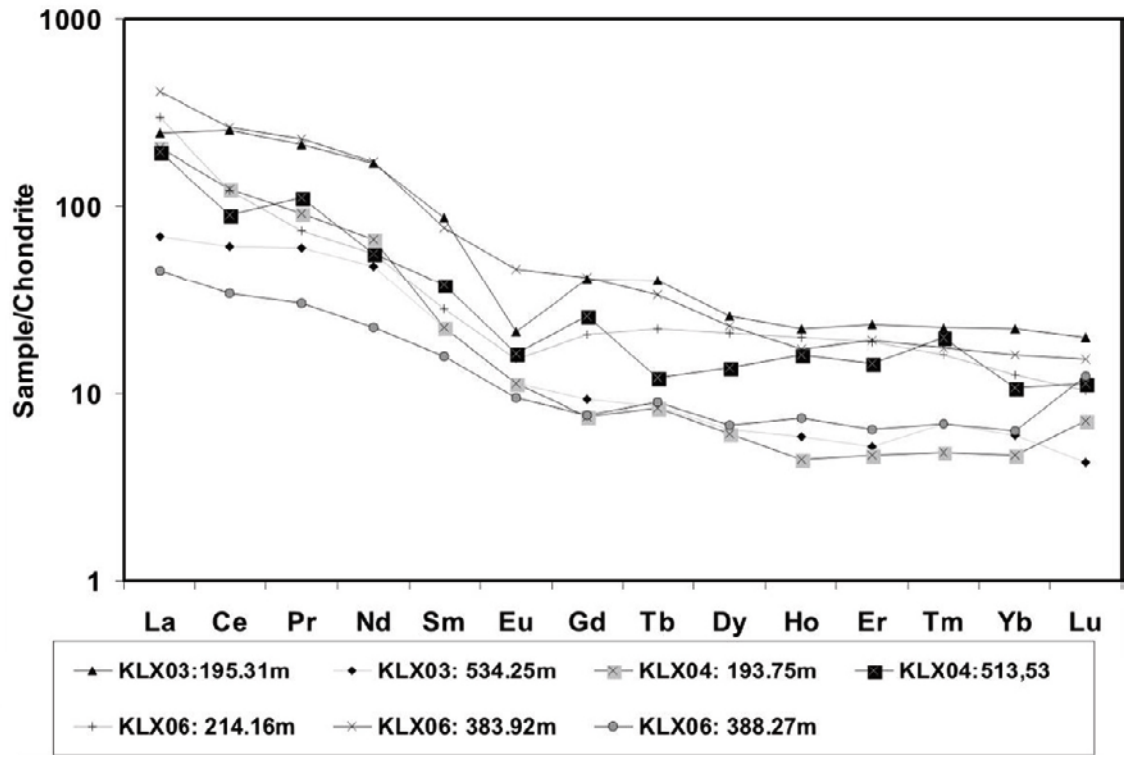

Figure 5-1. *Chondrite-normalised REE-values from samples from KLX03, KLX04 and KLX06 (Laxemar subarea). Chondrite values from /Evansen et al. 1978/.*

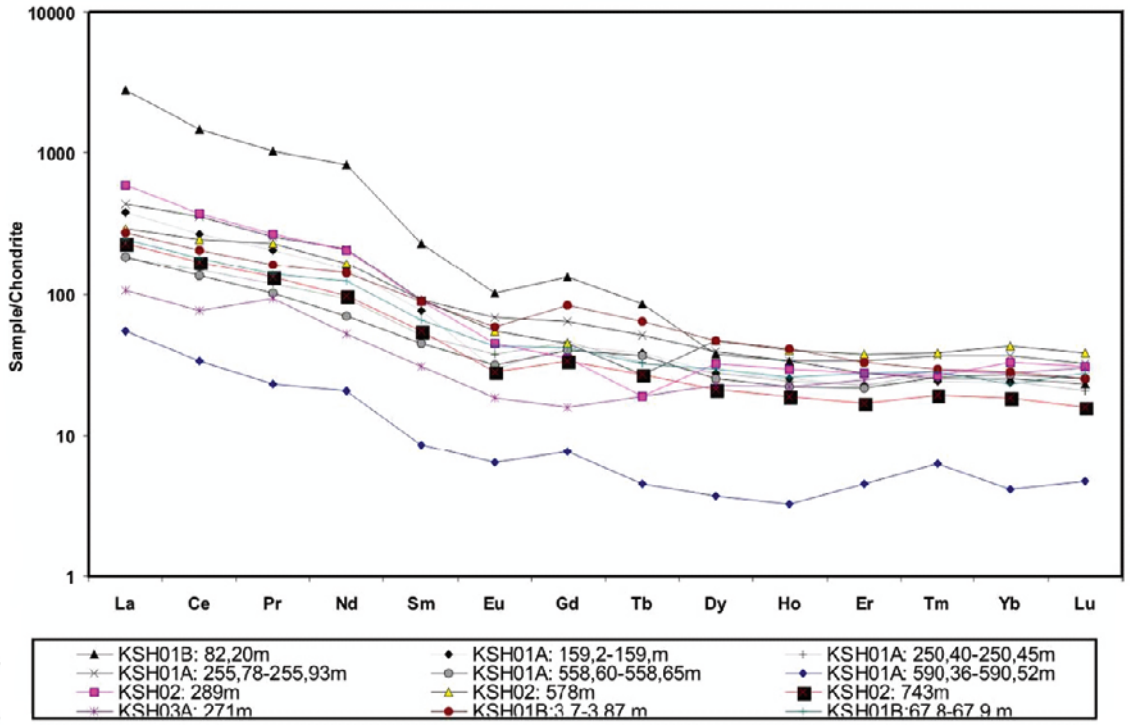

Figure 5-2. *Chondrite-normalised REE-values from samples from KSH01A+B, KSH02, and KSH03A (Simpevarp subarea). Chondrite values from /Evansen et al. 1978/.*

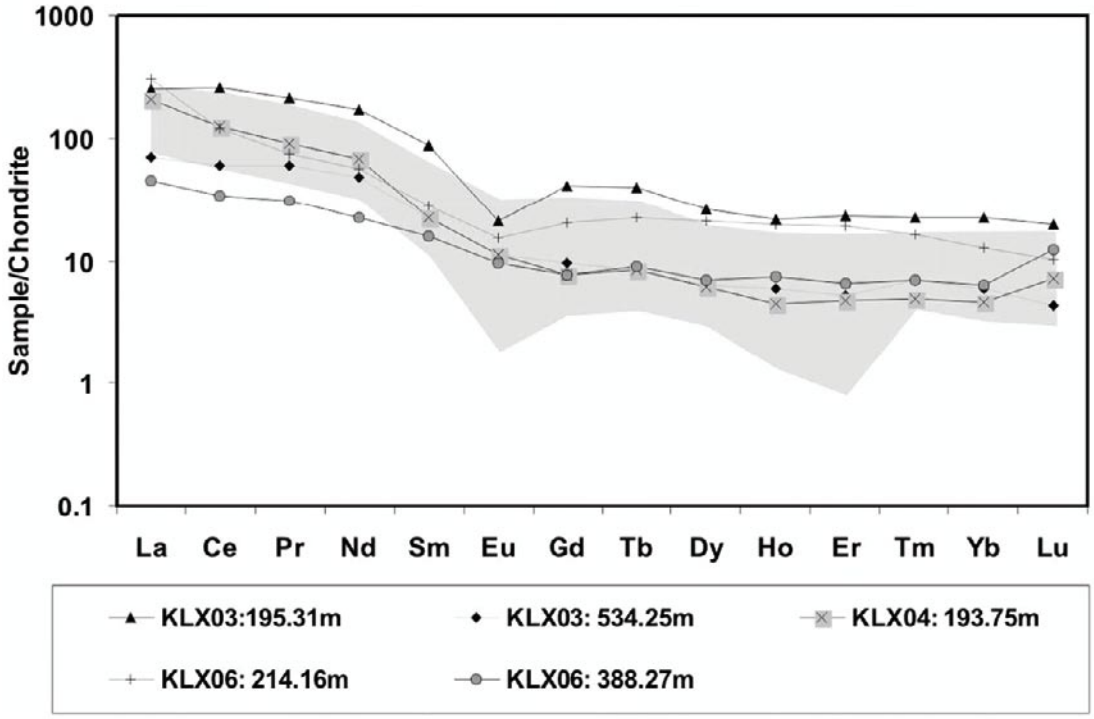

Figure 5-3. *Chondrite-normalised REE-values from samples with wall rock of Ävrö granite. Chondrite values from /Evansen et al. 1978/. Maximum and minimum REE-values from a large number of fresh Ävrö granite samples are shown by shading /Drake et al. 2006 and references therein/.*

However, sample KSH01B: 82.2 m has significantly higher LREE values than the other samples and may be due to contamination by REE-carbonate or possibly association of REE with organic matter, as suggested for similar patterns in fracture calcite at adjacent Äspö /Tullborg 2004/. Redox sensitive elements Ce and Eu are only depleted in a couple of samples (Ce – minor depletion in e.g. KLX04: 513.53–513.70 m and Eu depletion in e.g. KLX03: 195.36–195.36 m, KLX04: 513.53–513.70 m and KLX06: 214.11–214.16 m).

5.3 $\delta^{13}C$ and $\delta^{18}O$

In order to provide paleohydrogeological information 22 samples from KLX03 and 14 samples from KLX04, Laxemar subarea, have been analysed for $\delta^{13}C$ and $\delta^{18}O$ in calcite. Results from these analyses are shown in Appendix 3. Results from five KSH02 samples, Simpevarp subarea, are shown in Appendix 8.

The calcites are sampled from open or partly open fractures. In some open fractures it has been possible to sample calcites grown in open space showing euhedral crystal forms. Notations have been made on crystal morphology when possible since correspondence between calcite morphology (long and short c-axis) and groundwater salinity has been found in studies e.g. in Sellafield /Milodowski et al. 1998/. The impression from the Sellafield study is that carbonates precipitated from fresh water usually show short c-axis (nailhead shaped crystals) whereas calcite precipitated from saline waters preferably show long c-axis (scalenohedral shapes). Equant crystals are common in transition zones of brackish water. Concerning the samples from depth between 129–970 m, most of the samples with observable crystals shapes show equant to scalenohedral forms. Some crystals are needle shaped (from 105–267 m vertical depth) and some are identified as “short c-axis” (107, 624 and 913 m vertical depth).

The $\delta^{13}C$ and $\delta^{18}O$ values for the KLX03 and KLX04 calcites are plotted together with previously analysed calcites from subareas of Äspö, Laxemar and Simpevarp (Figure 5-4 and Figure 5-5). The KLX03 and KLX04 calcites show $\delta^{18}O$ values ranging from –6.3 to –19.4‰ and $\delta^{13}C$ values from –65.7 to –3.9‰. One calcite sample shows the lowest $\delta^{18}O$ (–19.4‰) value and has the highest $\delta^{13}C$ (–3.9‰) value, typical for hydrothermal calcites without signs of biogenic carbon. The other calcites have higher $\delta^{18}O$ values (indicating possible precipitates from meteoric or brackish Baltic Sea water based on fractionation factors by /O'Neil et al. 1969/ and ambient temperatures in the range of 7–15°C). These calcites also show larger spread in their $\delta^{13}C$ carbon isotope values supporting interaction with biogenic carbon. Extreme $\delta^{13}C$ values (as low as –65.7‰) indicate biogenic activity in the groundwater aquifers causing disequilibria in situ. It should be noted that the fractionation between HCO_3^- and $CaCO_3$ is only a few per mille and the $\delta^{13}C$ value in the calcite therefore largely reflects the composition in the bicarbonate at the time of calcite formation.

No calcites with $\delta^{18}O$ values around –12 to –14‰, interpreted as "warm brine" precipitates /Bath et al. 2000, Tullborg 2004/ have been recorded.

Four of the five calcite samples from KSH02 analysed for $\delta^{13}C$ and $\delta^{18}O$ show $\delta^{18}O$ of between –8.63 to –6.63‰ (from 100–420 m depth), which indicates that they might be precipitated from meteoric (or brackish Baltic Sea) water based on fractionation factors by /O'Neil et al. 1969/ and ambient temperatures in the range of 7–15°C. These samples also have $\delta^{13}C$ signatures (–14 to –10.3‰) suggesting an organic influence. A deeper sample show lower $\delta^{18}O$ (–11.5‰) and less distinct organic $\delta^{13}C$ signature (–7‰).

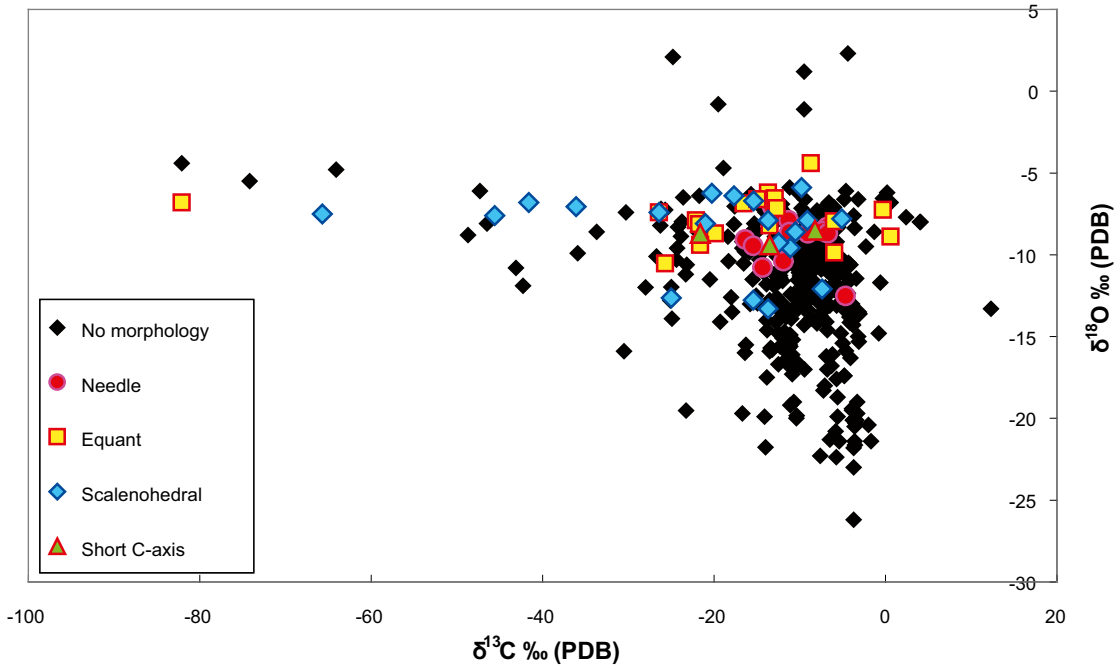

Figure 5-4. *$\delta^{13}C$ and $\delta^{18}O$ plot of calcite with different crystal shapes from the subareas Äspö, Simpevarp and Laxemar /Wallin and Peterman 1999, Bath et al. 2000, Drake and Tullborg 2004, 2006a, Milodowski et al. 2005, and this report/. Black symbols are samples without defined crystal morphology.*

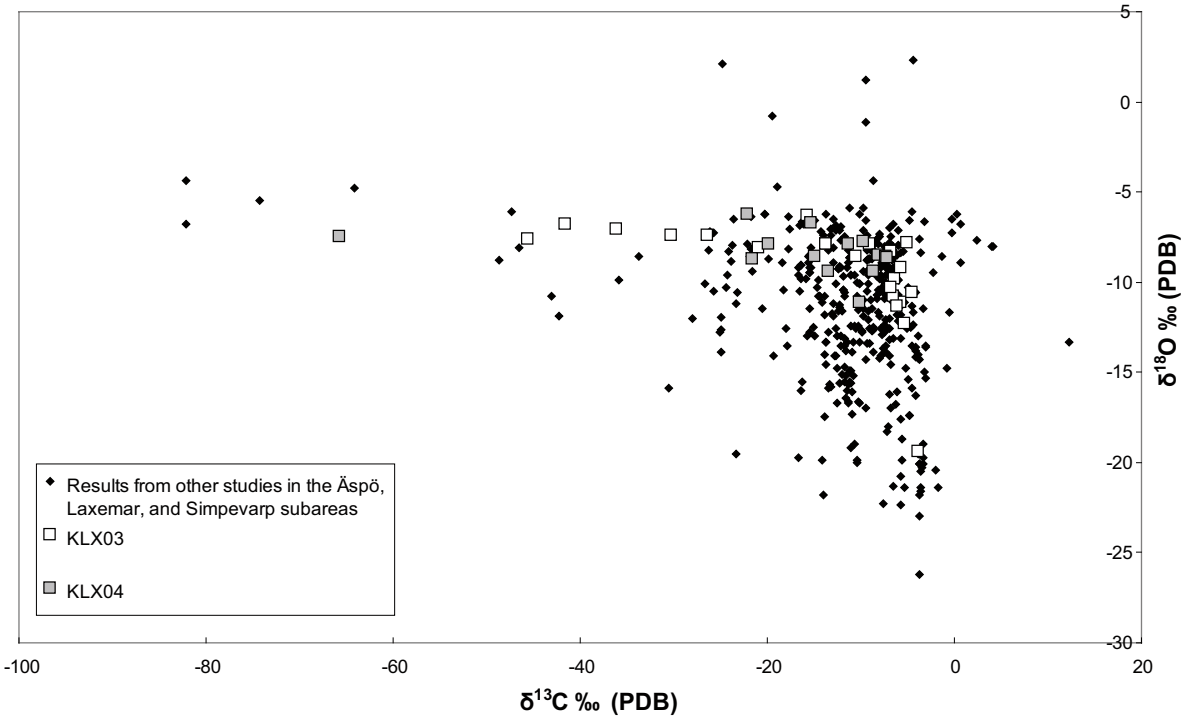

Figure 5-5. $\delta^{13}C$ and $\delta^{18}O$ *plot of calcite from KLX03 and KLX04 along with calcite from the subareas Äspö, Simpevarp (KSH01A+B, KSH02, KSH03A+B) and Laxemar /Wallin and Peterman 1999, Bath et al. 2000, Drake and Tullborg 2004, 2006a, Milodowski et al. 2005/.*

Figures 5-6 and 5-7 show $\delta^{18}O$ and $\delta^{13}C$ plotted versus depth for KLX03 and KLX04 along with calcites from other studies from subareas of Laxemar, Äspö and Simpevarp /Wallin and Peterman 1999, Bath et al. 2000, Drake and Tullborg 2004, 2006a, Milodowski et al. 2005/. These plots indicate that fractures in the upper 400 meters have been more open to low temperature circulation (possible interaction with Meteoric/Baltic sea water) and that calcites with carbon of biogenic origin, are common down to 300 m or more. However, stable isotopes in calcite suggest that low temperature circulation might have been active as deep as 967 m in KLX04 and 748 m in KLX03. For KLX04 the distribution of stable isotope values in calcite versus depth is in agreement with the flow logging results showing high hydraulic conductivity at e.g. 350 and 967 m. For KLX04 the distribution of calcite isotope values versus depth is in agreement with the flow logging results showing high hydraulic conductivity at e.g. 409 m, 457 m, 662 m and 772 m, respectively, while flowing sections are lacking at e.g. 130 m.

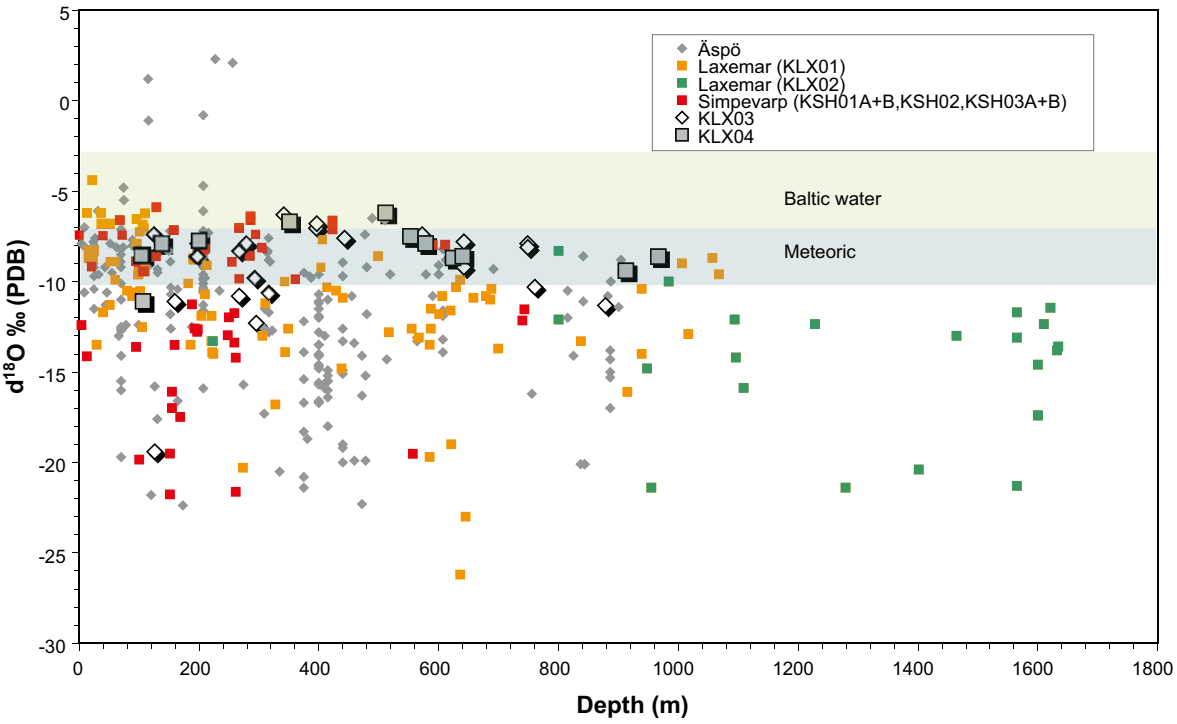

Figure 5-6. *Plot of $\delta^{18}O$ vs. depth (calcite) with samples from KLX03 and KLX04 along with calcite from the subareas Äspö, Simpevarp (KSH01A+B, KSH02, KSH03A+B) and Laxemar /Wallin and Peterman 1999, Bath et al. 2000, Drake and Tullborg 2004, 2006a, Milodowski et al. 2005 and this report/. Range of calcite precipitated from waters similar to the present Baltic Seawater and meteoric water at ambient temperatures is indicated - based on fractionation factors by /O'Neil et al. 1969/ and groundwater data from /SKB 2006/.*

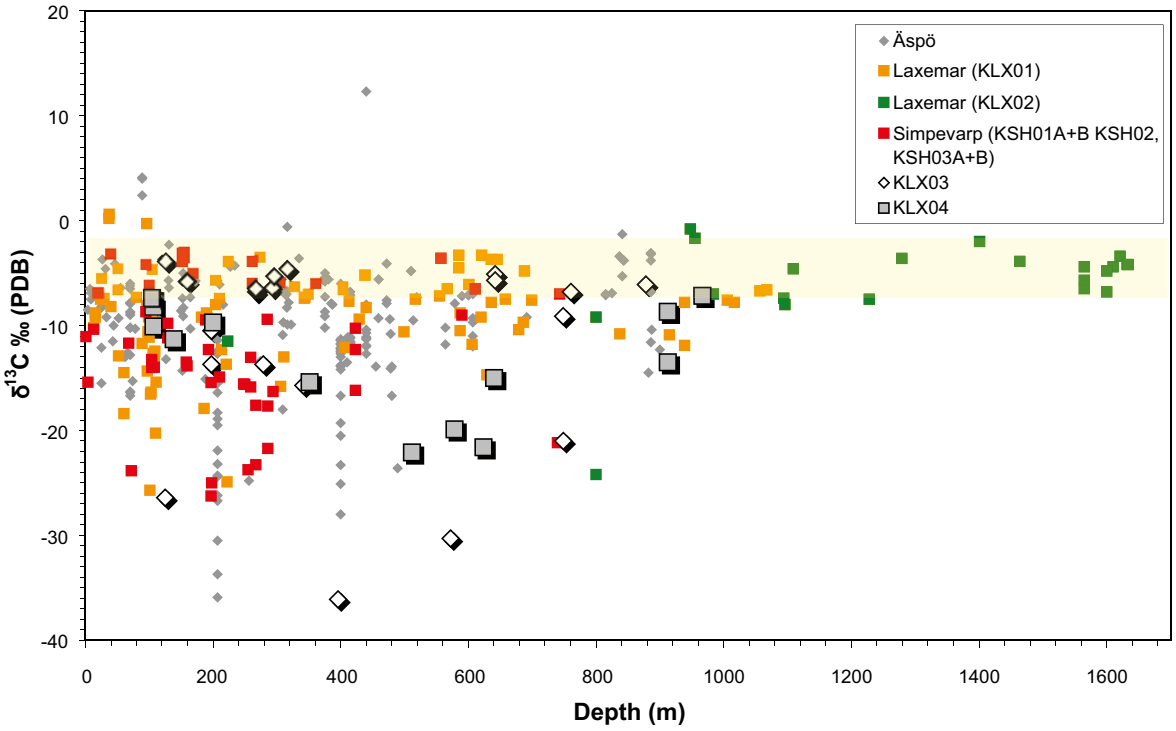

Figure 5-7. *Plot of $\delta^{13}C$ vs. depth (calcite) with samples from KLX03 and KLX04 along with calcite from the subareas Äspö, Simpevarp (KSH01A+B, KSH02, KSH03A+B) and Laxemar /Wallin and Peterman 1999, Bath et al. 2000, Drake and Tullborg 2004, 2006a, Milodowski et al. 2005 and this report/. The shaded area indicates the range of hydrothermal inorganic CO_3 /Drake and Tullborg 2007/.*

5.4 U-series

Results of the uranium decay series analyses are presented in Appendix 4, Appendix 6, and in Figures 5-8 and 5-9. Seven samples from KLX03, five samples from KLX04, three samples from KLX06, ten samples from KSH01A+B, three samples from KSH02 and one from KSH03A have been analysed. Comparison of these U and Th values with the ICP analyses of U and Th shows largely similar values (especially for U), suggesting that samples are relatively homogeneous.

The $^{234}U/^{238}U$ activity ratios vary between 0.7 and 3 and only a minor part of the samples show values close to 1 (Figure 5-8). The $^{230}Th/^{234}U$ activity ratios vary between 0.6 and 2.7 (Figure 5-8). The Thiel diagram of uranium decay (Figure 5-7, /Thiel et al. 1983/) also show that most samples show mobilisation or U during the last 300 ka (either deposition or removal) and many samples plot in the field for complex processes indicating that both mobilisation and deposition have occurred. Relatively few samples have values close to secular equilibria. A compilation of all the U-series analyses including thorough interpretation will be carried out at a later stage, in the background report for fracture mineralogy of the Simpevarp subarea.

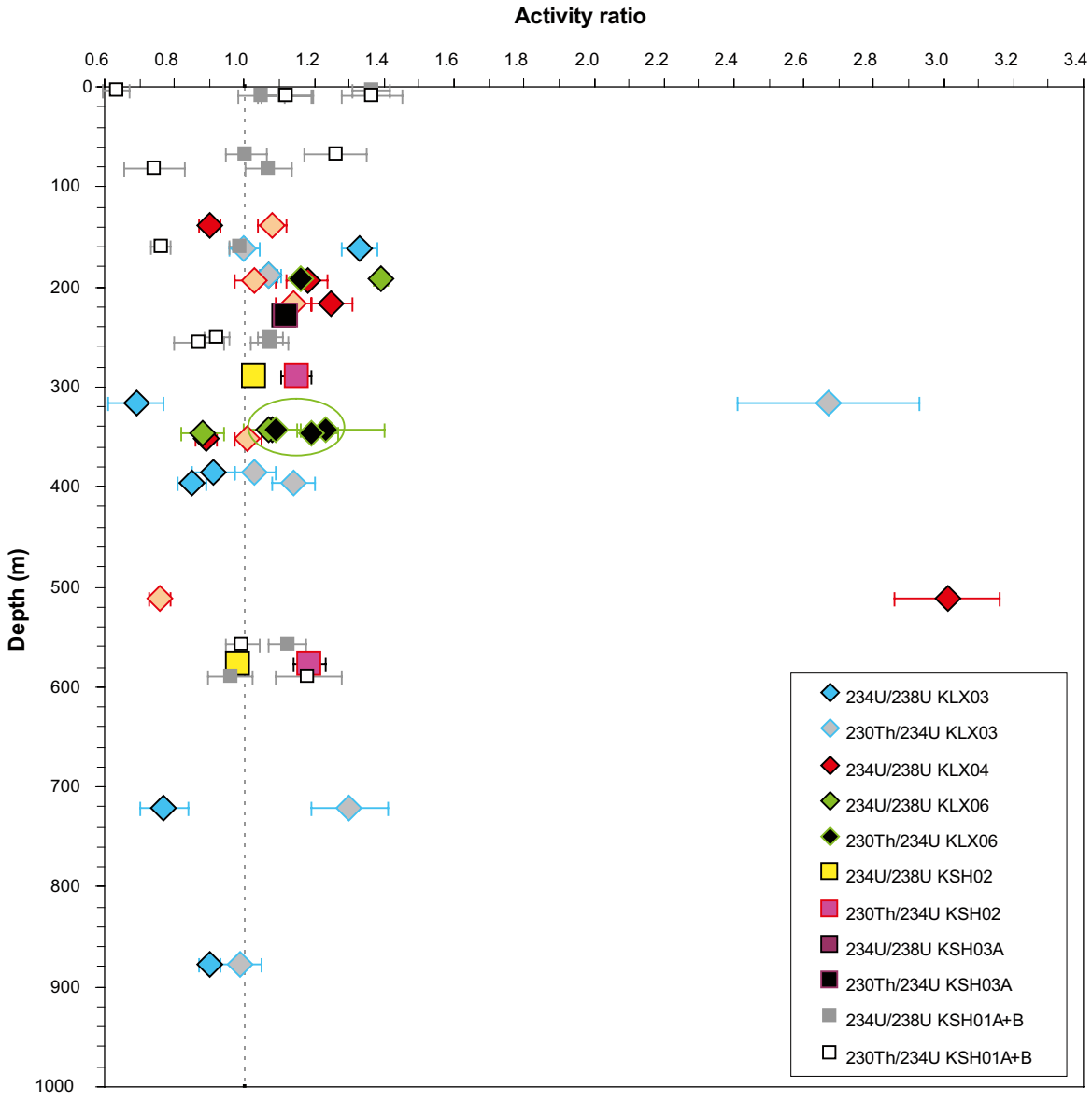

Figure 5-8. *Activity ratios of $^{234}U/^{238}U$ and $^{230}Th/^{234}U$ (with errors) vs. depth for fracture coating samples. One re-analysed sample is shown within an ellipse.*

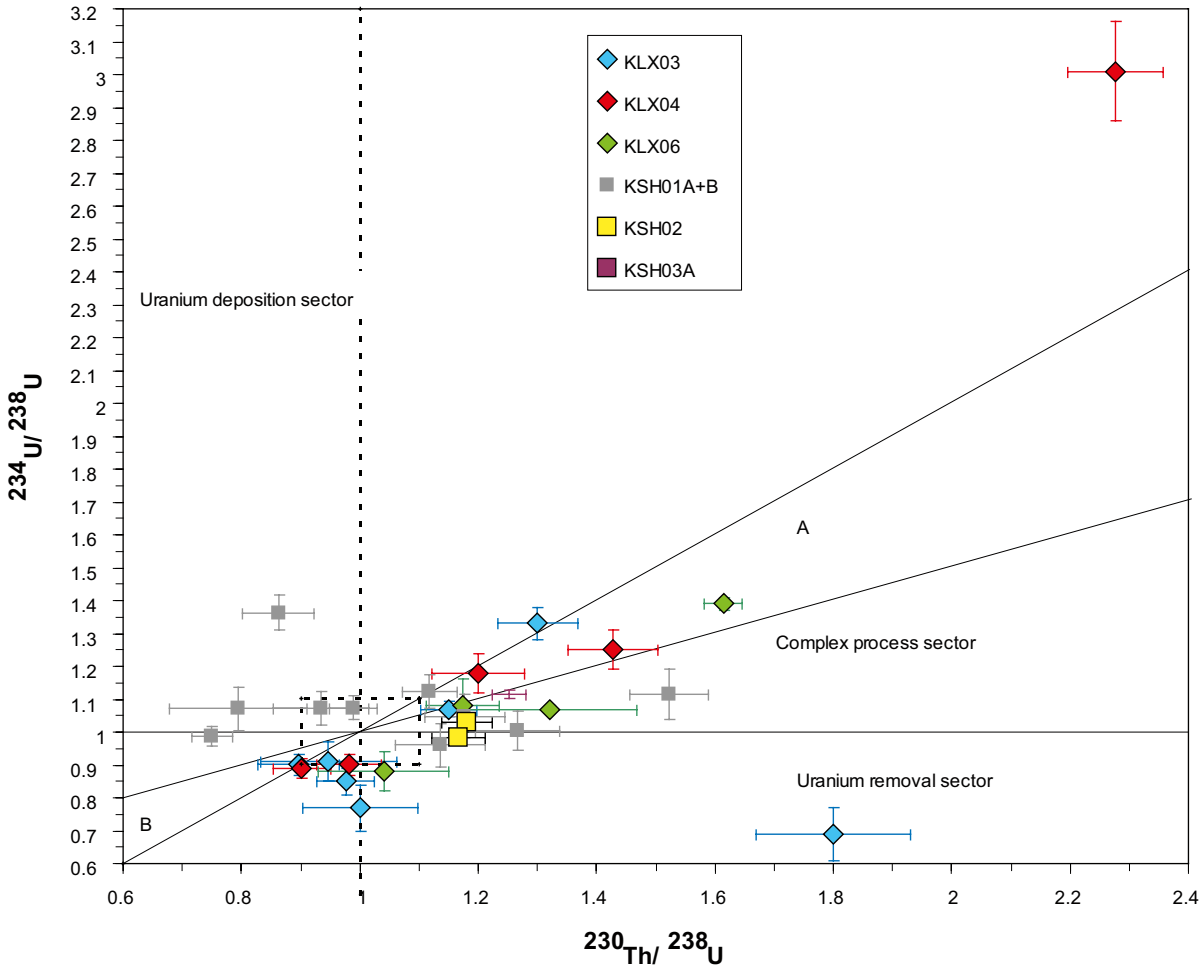

Figure 5-9. *Thiel diagram of uranium decay series with errors (after /Thiel et al. 1983/). A and B are forbidden sections for any single continuous process. Complex process sector is forbidden for any single process.*

6 Summary and discussions

In KLX03, the samples from the sections sampled for complete chemical characterisation (193.5–198.3 m, 408–415 m, 660–671 m, 735.5–748.03 m, 964–975 m) are dominated by chlorite, clay minerals (illite and mixed layer clay; e.g. corrensite), calcite, quartz, K-feldspar, plagioclase, hematite, pyrite and to a lesser degree by galena, barite, apatite, amphibole, mica, titanite and apophyllite. Quartz, K-feldspar, plagioclase, mica, titanite and most of the apatite are generally thought to be fragments from the wall rock incorporated into the fracture fillings, while chlorite, calcite, clay minerals, hematite, sulphides and barite are secondary. The sampled fractures are commonly re-activated older fractures, primary filled with e.g. epidote, calcite, chlorite, quartz, K-feldspar, hematite (and are sometimes cataclasites etc).

In KLX04, the samples from the sections sampled for complete chemical characterisation (103–213 m, 510–515 m, 971.21–976.21 m) are dominated by chlorite, clay minerals (illite and mixed layer clay; e.g. corrensite), calcite, quartz, K-feldspar, hematite, pyrite and to a lesser degree by apatite. Quartz and K-feldspar are generally thought to be fragments from the wall rock incorporated into the fracture fillings, while chlorite, calcite, clay minerals, hematite and pyrite are secondary. The mineralogy in samples from KLX06, KSH01A+B, KSH02 and KSH03A is generally similar to the mineralogy in samples from KLX03 and KLX04.

REE in the samples from KLX03 and KLX04 (in sections sampled for complete chemical characterisation) and in KLX06, KSH01A+B, KSH02 and KSH03A are very similar to REE in the host rock. Only one sample is significantly lower in Eu (KLX03:195.36–195.36 m). CaO contents are elevated compared to the host rock in calcite-rich samples. In clay mineral-rich samples, Fe, Mg and Al contents are higher than in the host rock, while the total values are lower (higher amount of crystal bound water) than in the host rock. One sample has a very high Ba content (15,400 ppm in KLX03:195.36–195.36 m). U concentrations in the two KLX03 samples are about 1 and 6 ppm.

$\delta^{18}O$ and $\delta^{13}C$ values in the sections sampled for complete groundwater characterisation are very similar to earlier sampled calcite from the subareas Laxemar, Simpevarp and Äspö. $\delta^{18}O$ is between –11 to –6.2‰, while most of the $\delta^{13}C$ values are between –10 and –5‰. However, three samples have very low $\delta^{13}C$ values (–22‰, –36‰ and –41‰ in samples KLX04: 513.53–513.70 m and KLX03: 409.83–410.13 m [2 samples]), indicating biogenic activity in the groundwater aquifers causing disequilibrium in situ. The calcite samples from KSH02 show no extreme $\delta^{18}O$ and $\delta^{13}C$ values.

The additional samples from KSH02 and KSH03A all belongs to gouge-rich sections in the bedrock and are dominated by chlorite, corrensite, illite and hematite in addition to the wall rock fragments (K-feldspar, quartz and plagioclase).

The U-series analyses from boreholes KLX03, KLX04, KLX06, KSH01A+B, KSH02 and KSH03A, show that U-mobilisation (deposition and/or removal) have taken place during the last 300,000 years in most of the samples. Possible disturbances caused by the drilling and subsequent handling of the drill cores can however not be ruled out. Further evaluation is planned for the background report for fracture mineralogy of the Simpevarp subarea.

7 References

Ask H, Morosini M, Samuelsson L-E, Ekström L, Håkanson N, 2005a. Oskarshamn site investigation. Drilling of cored borehole KLX03, SKB P-05-167, Svensk Kärnbränslehantering AB.

Ask H, Morosini M, Samuelsson L-E, Ekström L, Håkanson N, 2005b. Oskarshamn site investigation. Drilling of cored borehole KLX04, SKB P-05-111, Svensk Kärnbränslehantering AB.

Bath A, Milodowski A, Ruotsalainen P, Tullborg E-L, Cortés Ruiz A, Aranyossy J-F, 2000. Evidences from mineralogy and geochemistry for the evolution of groundwater systems during the quaternary for use in radioactive waste repository safety assessment (EQUIP project). EUR report 19613.

Drake H, Tullborg E-L, 2004. Oskarshamn site investigation. Fracture mineralogy and wall rock alteration. Results from drill core KSH01A+B, SKB-P-04-250, Svensk Kärnbränslehantering AB.

Drake H, Tullborg E-L, 2006a. Oskarshamn site investigation. Fracture mineralogy. Results from drill core KSH03A+B, P-06-03, Svensk Kärnbränslehantering AB. 65 pp.

Drake H, Tullborg E-L, 2006b. Oskarshamn site investigation. Mineralogical, chemical and redox features of red-staining adjacent to fractures. Results from drill core KLX04, P-06-02, Svensk Kärnbränslehantering AB.

Drake H, Tullborg E-L, 2006c. Oskarshamn site investigation. Mineralogical, chemical and redox features of red-staining adjacent to fractures. Results from drill cores KSH01A+B and KSH03A+B, P-06-01, Svensk Kärnbränslehantering AB. 115 pp.

Drake H, Tullborg E-L, 2007. Oskarshamn site investigation. Fracture mineralogy. Results from drill cores KLX03, KLX04, KLX06, KLX07A, KLX08 and KLX10A, SKB P-07-74, Svensk Kärnbränslehantering AB.

Drake H, Sandström B, Tullborg E-L, 2006. Mineralogy and geochemistry of rocks and fracture fillings from Forsmark and Oskarshamn: Compilation of data for SR-Can, SKB R-06-109, Svensk Kärnbränslehantering AB.

Drever S I, 1973. The preparation of oriented clay mineral specimens for X-ray diffraction analysis by a filter-membrane peel technique. American Mineralogist, 58, 553–554.

Evansen N M, Hamilton P J, O'Nions R K, 1978. Rare Earth Abundances in Chondritic Meteorites: Geochimica et Cosmochimica Acta, 42, 1199–1212.

Milodowski A E, Gillespie M R, Pearce J M, Metcalfe R, 1998. Collaboration with the SKB EQUIP programme; Petrographic characterisation of calcites from Äspö and Laxemar deep boreholes by scanning electron microscopy, electron microprobe and cathodoluminescence petrography, WG/98/45C: British Geological Survey, Keyworth, Nottingham.

Milodowski A E, Tullborg E-L, Buil B, Gomez P, Turrero M-J, Haszeldine S, England G, Gillespie M R, Torres T, Ortiz J E, Zacharias J, Silar J, Chvatal M, Strnad L, Sebek O, Bouch J E, Chenery S R, Chenery C, Shepherd T J, McKervey J A, 2005. Application of Mineralogical, Petrological and Geochemical tools for Evaluating the Palaeohydrogeological Evolution of the PADAMOT Study Sites, PADAMOT Project Technical Report WP2.

O'Neil J R, Clayton R N, Mayeda T K, 1969. Oxygen isotope fractionation in divalent metal carbonates: Journal of Chemistry and Physics, 51, 5547–5558.

PDF 1994. Powder diffraction file computer data base. International Centre for Diffraction Data, Park Lane, Swartmore, PA, USA, Set 1–43.

Rouhiainen P, Sokolnicki M, 2005. Oskarshamn site investigation. Difference flow logging of borehole KLX04. Subarea Laxemar, SKB P-05-68, Svensk Kärnbränslehantering AB.

Rouhiainen P, Pöllänen J, Sokolnicki M, 2005. Oskarshamn site investigation. Difference flow logging of borehole KLX 03. Subarea Laxemar, SKB P-05-67, Svensk Kärnbränslehantering AB.

SKB 2006. Hydrogeochemical evaluation, Preliminary site description Laxemar subarea – version 1.2, SKB-R-06-12, Svensk Kärnbränslehantering AB.

Sokolnicki M, Rouhiainen P, 2005. Difference flow logging in borehole KLX06. Subarea Laxemar. Oskarshamn site investigation, SKB P-05-74, Svensk Kärnbränslehantering AB.

Thiel K, Vorwerk R, Saager R, Stupp H D, 1983. ^{235}U fission tracks and ^{238}U-series disequilibria as a means to study Recent mobilization of uranium in Archaean pyritic conglome-rates: Earth and Planetary Science Letters, 65, 249–262.

Tullborg E-L, 2004. Palaeohydrogeological evidences from fracture filling minerals – Results from the Äspö/Laxemar area. Mat. Res. Soc. Symp. Vol 807, 873–878.

Wallin B, Peterman Z, 1999. Calcite fracture fillings as indicators of Paleohydrology at Laxemar at the Äspö hard rock laboratory, southern Sweden: Applied Geochemistry, volume 14:7, 939–952.

Appendix 1

Sample descriptions for samples from drill cores KLX03, KLX04 and KLX06

KLX03: 168.47–168.54 m

Minerals in old reactivated fractures (macroscopic): Chlorite, calcite, epidote, quartz and laumontite of several generations (cross-cutting). There are cataclastic parts as well (dominated by chlorite, K-feldspar, quartz and probably also some hematite). The wall rock is red-stained (due to hydrothermal alteration; alteration of plagioclase, biotite and magnetite and formation of secondary adularia, albite, chlorite, prehnite and hematite).

Minerals on the fracture surface according to XRD: Dominantly calcite, but also quartz, chlorite, illite and mixed layer-clay.

Photograph of drill core sample KLX03: 168.47–168.54 m.

Photograph of the fracture surfaces of drill core sample KLX03: 168.47–168.54 m.

KLX03: 195.36–195.36 m

Minerals in old reactivated fractures (macroscopic): Network of thin fractures with no visible filling. The wall rock is very faintly red-stained.

Minerals on the fracture surface (SEM-EDS, in order of abundance): Dominated by chlorite, calcite, mixed layer-clay with minor amounts of pyrite, quartz, illite, K-feldspar, hematite and titanite.

Minerals on the fracture surface according to XRD: Quartz, K-feldspar, albite, amphibole, chlorite, calcite and mixed layer-clay.

Photograph of the drill core sample KLX03: 195.36–195.36 m.

KLX03: 326.94–327.04 m

Minerals in old reactivated fractures (macroscopic): Calcite and chlorite of several generations (cross-cutting fractures with different orientations). The wall rock is red-stained as a consequence of hydrothermal alteration.

Minerals on the fracture surface (SEM-EDS, in order of abundance): Dominated by mixed layer-clay and pyrite (cubic) with smaller amounts of calcite and hematite.

Minerals on the fracture surface according to XRD: Calcite, plagioclase, quartz, chlorite and mixed layer-clay.

Photograph of drill core sample KX03: 326.94–327.04 m.

Photograph of the fracture surfaces of drill core sample KLX03: 326.94–327.04 m.

Back-scattered SEM-image of pyrite (bright cubic crystals) calcite (arrows) and mixed-layer clay (the rest). Sample KLX03: 326.94–327.04 m.

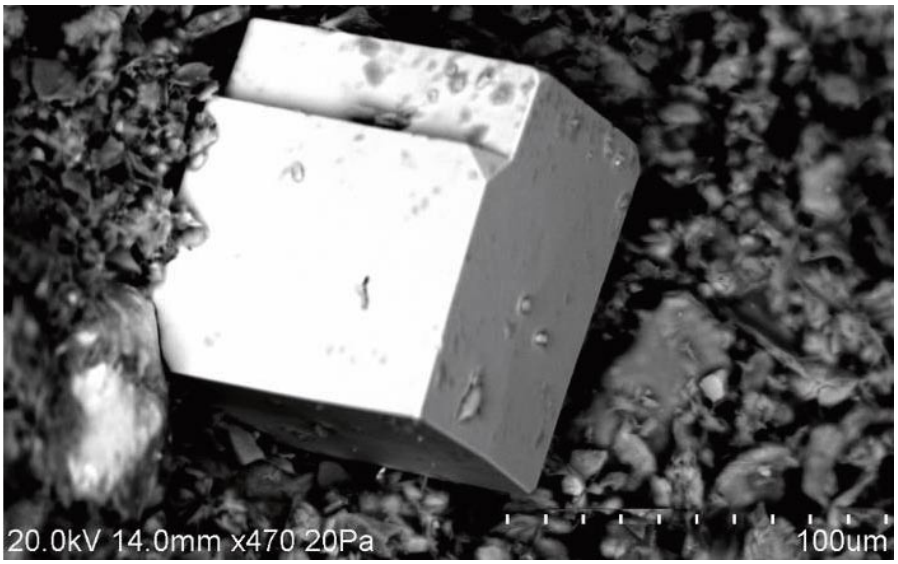

Back-scattered SEM-image of cubic pyrite (bright) and mixed-layer clay. Sample KLX03: 326.97–327.04 m.

KLX03: 397.79–397.89 m

Minerals in old reactivated fractures (macroscopic): Chlorite, calcite, epidote and quartz (possibly also prehnite). The fracture filed with these minerals is cut by several younger fractures. The wall rock is red-stained.

Minerals on the fracture surface (SEM-EDS, in order of abundance): Mixed layer-clay, wall rock fragments (e.g. quartz, plagioclase and titanite), calcite, and small amounts of hematite, barite, pyrite and an unidentified Zn-rich mineral.

Minerals on the fracture surface according to XRD: Calcite, quartz, K-feldspar, chlorite and mixed layer-clay.

Photograph of drill core sample KLX03: 397.79–397.89 m.

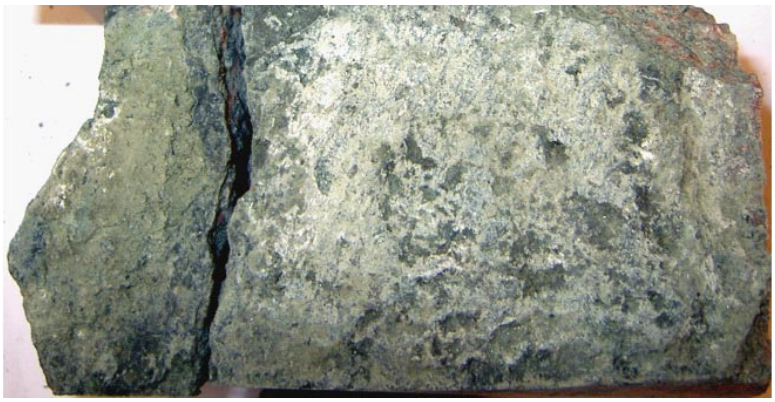

Photograph of one fracture surface of drill core sample KLX03: 397.79–397.89 m.

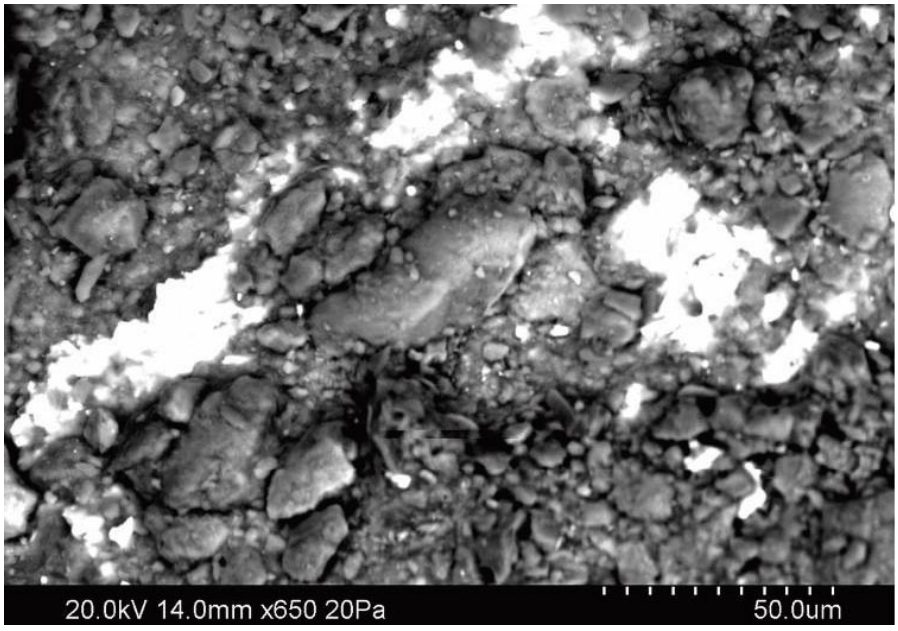

Back-scattered SEM-image of barite (bright) and mixed-layer clay (the rest; mostly covering wall rock fragments). Sample KLX03: 397.79–397.89 m.

KLX03: 409.83–410.13 m

Minerals in old reactivated fractures (macroscopic): Very thin calcite coating on the fracture which runs sub-parallel to the borehole. Wall rock is very faintly red-stained up to a centimetre away from the fracture. The other fractures have lower amounts of fracture coatings.

Minerals on the fracture surface (SEM-EDS, in order of abundance): Dominated by calcite (scalenohedral crystals), barite, chlorite, corrensite and illite with minor amounts of pyrite, K-feldspar, quartz, and trace amounts of biotite and apatite.

Minerals on the fracture surface according to XRD: Quartz, plagioclase, K-feldspar, calcite, chlorite, mica and mixed layer-clay.

Photograph of drill core sample KLX03: 409.83–410.13 m.

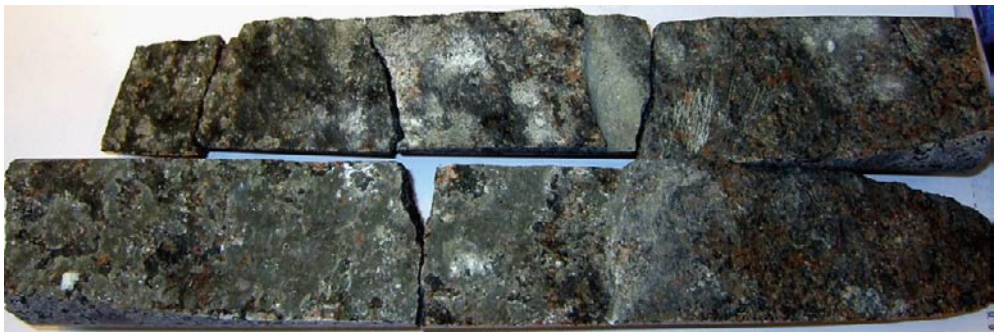

Photograph of the fracture surfaces of drill core sample KLX03: 409.83–410.13 m.

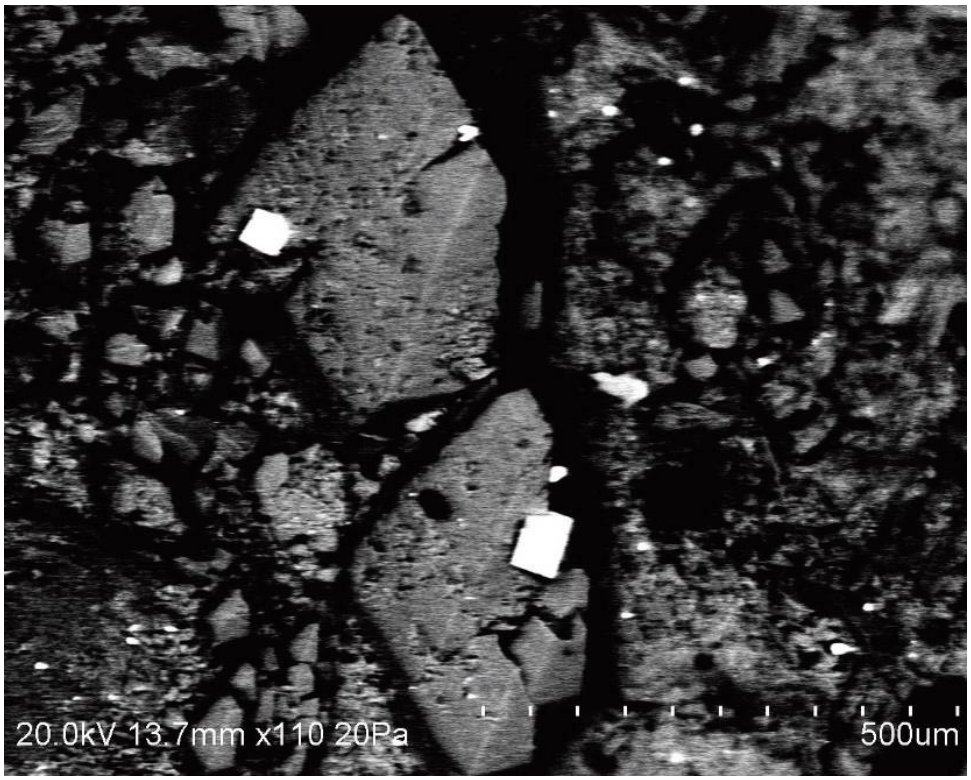

Back-scattered SEM-image of pyrite (bright cubic crystals) and scalenohedral calcite (c-axis elongated and partly dissolved crystals). Sample KLX03: 409.83–410.13 m.

KLX03: 534.25–534.40 m

Minerals in old reactivated fractures (macroscopic): None. Fresh wall rock (at least no macroscopically visible alteration). This sample is from a section characterized by low fracture frequencies.

Minerals on the fracture surface (macroscopic): Gypsum.

Photograph of drill core sample KLX03: 534.25–534.40 m. Gypsum have been scraped off from parts of the fracture surface.

KLX03: 662.33–662.65 m

Minerals in old reactivated fractures (macroscopic): Thick reactivated calcite filled fracture. At least two generations of calcite is present in this sample.

Minerals on the fracture surface (SEM-EDS, in order of abundance): Dominated by calcite (scalenohedral crystals), barite (occasionally Euhedral crystals), and pyrite (occasionally cubic crystals) with minor amounts of quartz, chlorite and galena.

Minerals on the fracture surface according to XRD: Calcite, quartz, K-feldspar, chlorite, barite, and mixed layer-clay.

Photograph of drill core sample KLX03: 662.33–662.65 m.

Photograph of the fracture surfaces of drill core sample KLX03: 662.33–662.65 m.

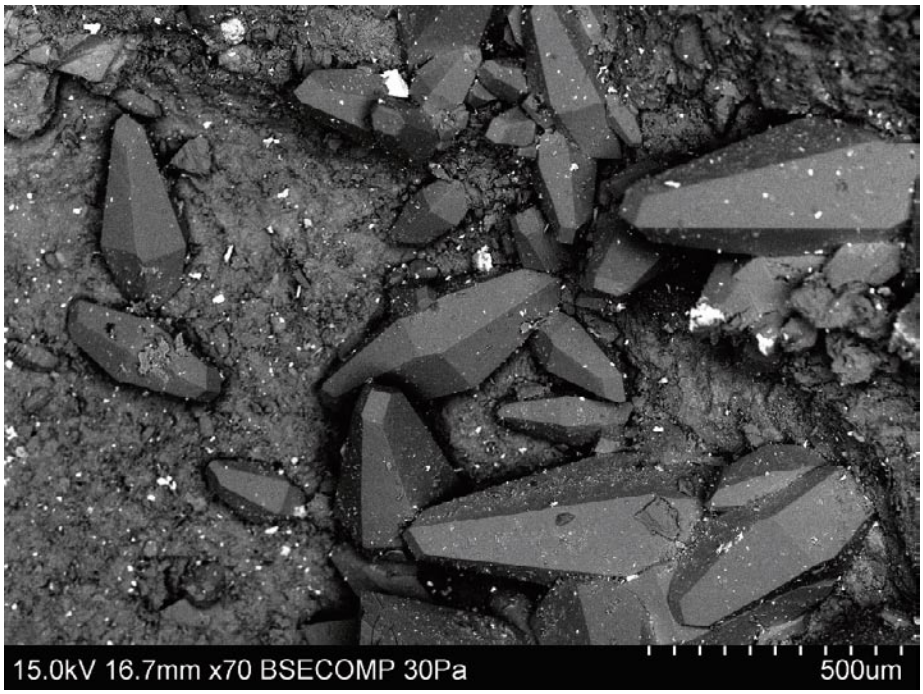

Back-scattered SEM-image of scalenohedral calcite crystals and barite (bright crystals). Sample KLX03: 662.33–662.65 m.

KLX03: 743.98–744.06 m

Minerals in old reactivated fractures (macroscopic): A one centimetre wide filling made up of minerals formed at several events; chlorite, calcite, epidote, adularia, quartz, laumontite, prehnite, hematite and pyrite. The wall rock is red-stained and this alteration is occasionally intensified towards the fracture.

Minerals on the fracture surface (SEM-EDS, in order of abundance). Mixed layer-clay, calcite, hematite and small amounts of galena.

Minerals on the fracture surface according to XRD: Calcite, chlorite, K-feldspar, corrensite and mixed layer-clay.

Photograph of drill core sample KLX03: 743.98–744.06 m.

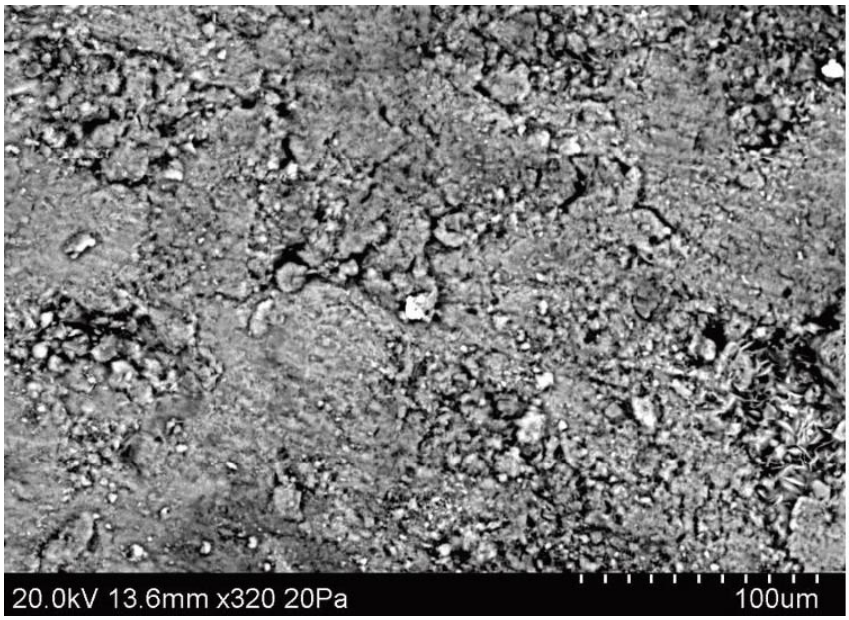

Back-scattered SEM-image of mixed layer-clay (dominates) and hematite (bright crystals). Sample KLX03: 743.98–744.06 m.

KLX03: 904.38–904.54 m

Minerals in old reactivated fractures (macroscopic): Cataclasite including e.g. epidote and chlorite. This section is highly fractured but most fractures are sealed with very thin mineral fillings. The wall rock is red-stained.

Minerals on the fracture surface (SEM-EDS, in order of abundance): Mixed layer-clay, illite, quartz, calcite, hematite and galena.

Minerals on the fracture surface according to XRD: Quartz, K-feldspar, plagioclase, calcite, chlorite, illite and mixed layer-clay.

Photograph of drill core sample KLX03: 904.38–904.54 m.

Photograph of one fracture surface of drill core sample KLX03: 904.38–904.54 m.

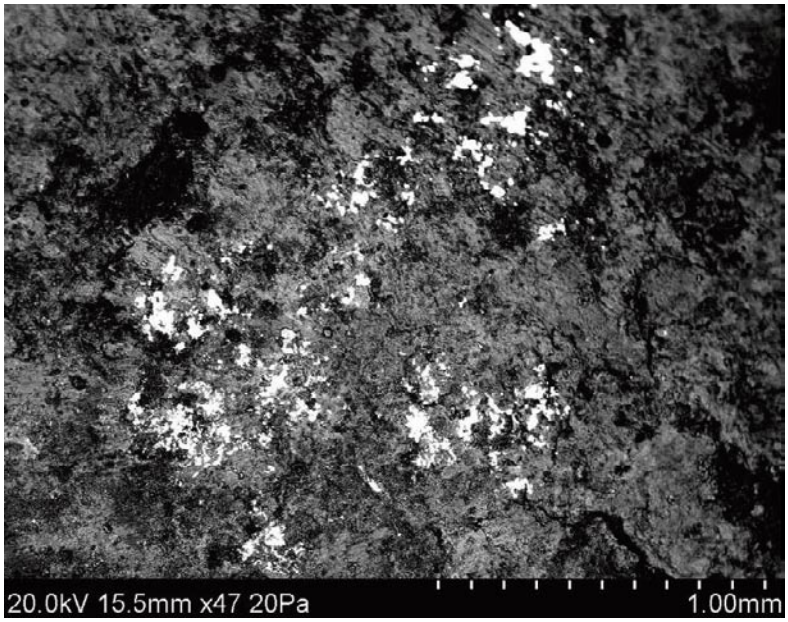

Back-scattered SEM-image of mixed layer-clay and galena (bright crystals). Sample KLX03: 904.38–904.54 m.

KLX03: 969.21–969.27 m

Minerals in old reactivated fractures (macroscopic): Sealed network of fractures filled with dominantly (in order) prehnite, epidote, pyrite and fluorite. The wall rock is intensively red-stained.

Minerals on the fracture surface (SEM-EDS, in order of abundance): Apophyllite, mixed layer-clay, prehnite, apatite and plagioclase.

Photograph of drill core sample KLX03: 969.21–969.27 m. The fractures shown are dominantly filled with prehnite.

Photograph of the fracture surfaces of drill core sample KLX03: 969.21–969.27 m.

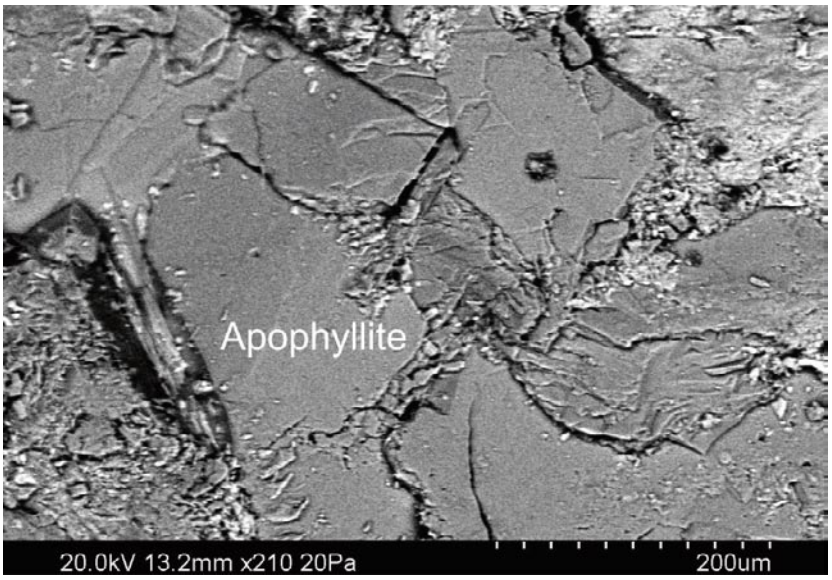

Back-scattered SEM-image of apophyllite. Sample KLX03: 969.21–969.27 m.

KLX04: 139.08–139.13 m

Minerals in old reactivated fractures (macroscopic): Sealed network of thin fractures without visible fillings. The wall rock is red-stained in the whole sample.

Photograph of drill core sample KLX04:139.08– 139.13 m.

KLX04: 193.74–193.90 m

Minerals in old reactivated fractures (macroscopic): Cataclasite, epidote, K-feldspar, chlorite, hematite, quartz, (calcite). These fractures may be of several generations. The wall rock is red-stained as a consequence of hydrothermal alteration.

Minerals on the fracture surface (SEM-EDS, in order of abundance): Illite, mixed-layer clay (most probably of corrensite-type), chlorite, hematite, pyrite and apatite.

Minerals on the fracture surface according to XRD: Quartz, K-feldspar, chlorite, calcite and mixed layer-clay.

Photograph of drill core sample KLX04: 193.74–193.90 m.

KLX04: 216.66–216.79 m

Minerals in old reactivated fractures (macroscopic): Epidote, chlorite and possibly laumontite, calcite and quartz. The wall rock is intensively red-stained as a consequence of hydrothermal alteration.

Minerals on the fracture surface according to XRD: Quartz, K-feldspar, plagioclase, chlorite and mixed layer-clay.

Photograph of drill core sample KLX04: 216.66–216.79 m.

KLX04: 352.69–352.81 m

Minerals in old reactivated fractures (macroscopic): Cataclasite made up of chlorite, K-feldspar, hematite and wall rock fragments (K-feldspar, quartz and plagioclase etc).

Minerals on the fracture surface (SEM-EDS, in order of abundance): Illite, mixed layer-clay (Mg-rich), chlorite, calcite, K-feldspar, hematite, and small amounts of pyrite, galena, as well as an unidentified U-rich silicate.

Minerals on the fracture surface according to XRD: Calcite, quartz, K-feldspar, plagioclase, chlorite, illite and mixed layer-clay.

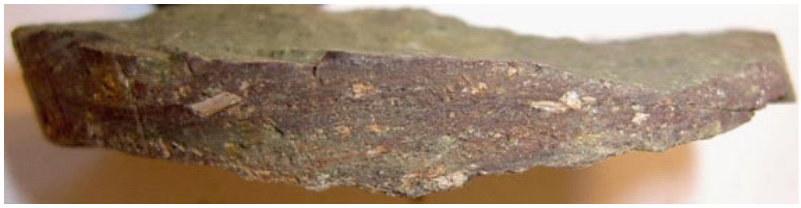

Photograph of the drill core sample KLX04: 352.69–352.81 m.

Photograph of the fracture surfaces of the drill core sample KLX04: 352.69–352.81 m.

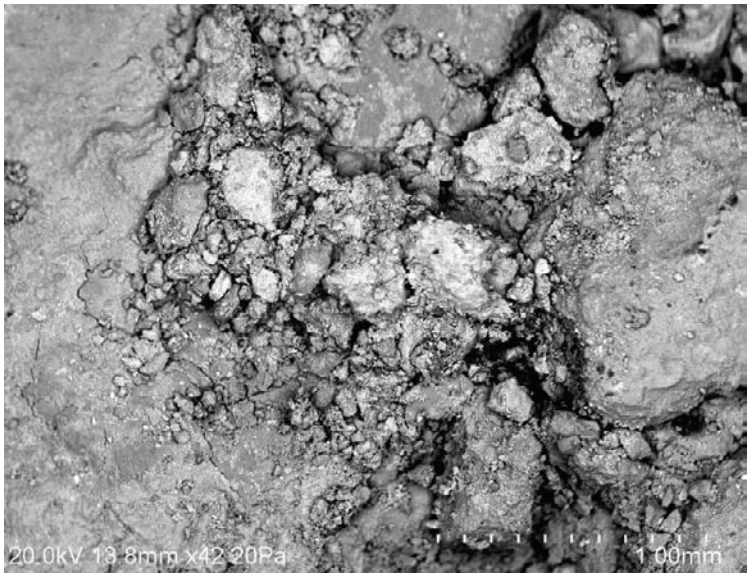

Back-scattered SEM-image of mixed-layer clay (bright parts) and illite (grey).
From sample KLX04: 352.69–352.81 m.

KLX04: 513.53–513.70 m

Minerals in old reactivated fractures (macroscopic): Chlorite, calcite, quartz, K-feldspar and possibly biotite. The wall rock is red-stained. The fracture is found in the contact between two different rock types.

Minerals on the fracture surface (macroscopic): Clay minerals, chlorite, pyrite and calcite.

Photograph of drill core sample KLX04: 513.53–513.70 m.

Photograph of the fracture surfaces of drill core sample KLX04: 513.53–513.70 m.

KLX06: 214.11–214.16 m

Minerals in old reactivated fractures (macroscopic): Cataclasite (chlorite, K-feldspar, hematite and wall rock fragments) and pyrite. The wall rock is heavily red-stained due to hydrothermal alteration (affecting mainly plagioclase, biotite and magnetite).

Minerals on the fracture surface (SEM-EDS, in order of abundance): Mixed layer-clay (of unknown composition), illite, fluorite, K-feldspar, quartz, albite, REE-carbonate, hematite and trace amounts of calcite.

Minerals on the fracture surface according to XRD: Fluorite, quartz, K-feldspar, albite, chlorite and mixed layer-clay.

Photograph of drill core sample KLX06: 214.11–214.16 m.

Photograph of the fracture surfaces of drill core sample KLX06: 214.11–214.16 m.

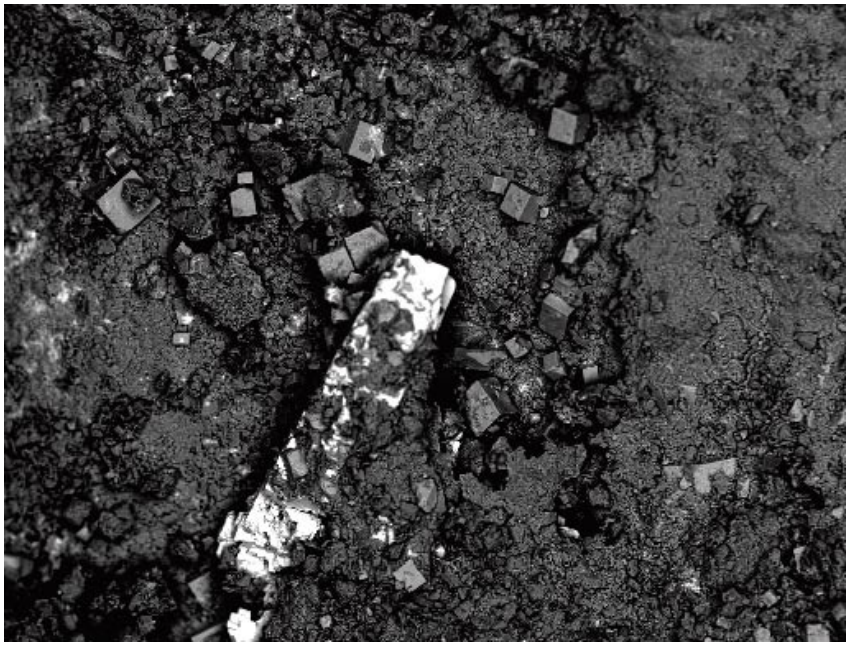

Back-scattered SEM-image of pyrite (bright), fluorite (cubic crystals) and mixed layer-clay (the dominant part of the coating). Width of view is about 600 µm. Sample KLX06: 214.11–214.16 m.

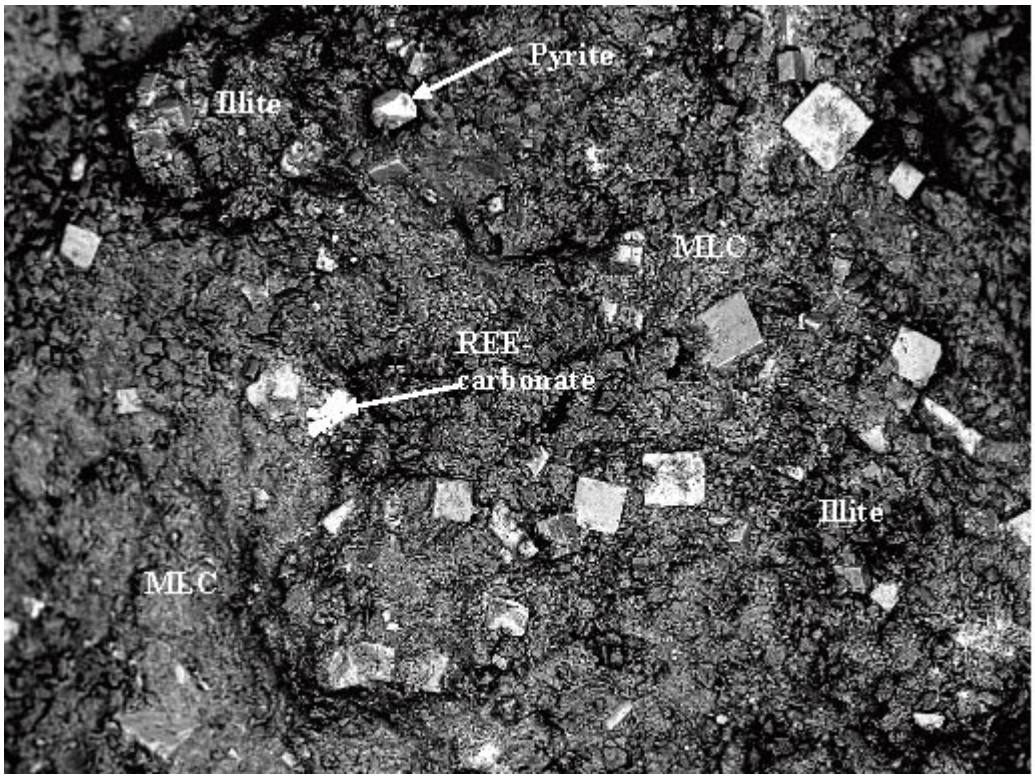

Back-scattered SEM-image of pyrite, fluorite (cubic crystals), REE-carbonate and mixed layer-clay (MLC) and illite. Width of view is about 600 µm. Sample KLX06: 214.11–214.16 m.

KLX06: 383.93–383.93 m

Minerals in old reactivated fractures (macroscopic): Cataclasite consisting of chlorite, clay minerals, K-feldspar, hematite and wall rock fragments.

Minerals on the fracture surface (SEM-EDS, in order of abundance): Mixed layer-clay, hematite (small crystals in the mixed-layer clay), illite, pyrite and wall rock fragments (e.g. zircon).

Minerals on the fracture surface according to XRD: Quartz, K-feldspar, albite, chlorite, epidote and hematite.

Photograph of drill core sample KLX06: 383.93–383.93 m.

Photograph of one of the fracture surfaces of drill core sample KLX06: 383.93–383.93 m.

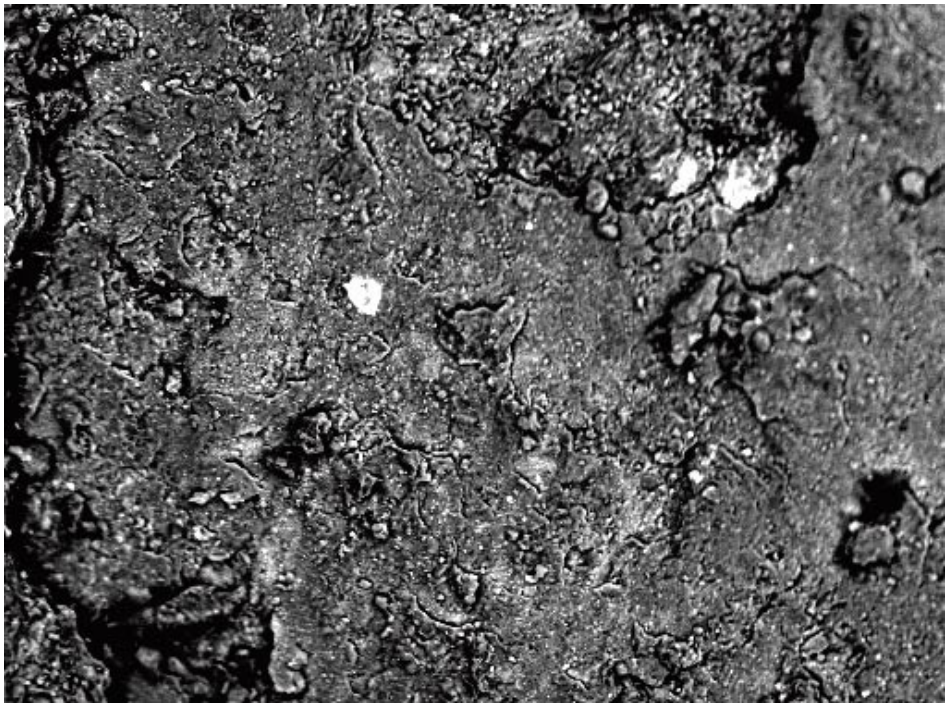

Back-scattered SEM-image of mixed layer-clay (grey) and hematite (bright crystals). Width of view is about 600 µm. Sample KLX06: 383.93–383.93 m.

KLX06: 388.27–388.30 m

Minerals in old reactivated fractures (macroscopic): Cataclasite (chlorite, clay minerals, K-feldspar, hematite and wall rock fragments), laumontite and possibly calcite.

Minerals on the fracture surface (SEM-EDS, in order of abundance): Illite, hematite and mixed-layer clay.

Minerals on the fracture surface according to XRD: Quartz, K-feldspar, muscovite, mixed layer-clay (and epidote).

Photograph of drill core sample KLX06: 388.27–388.30 m.

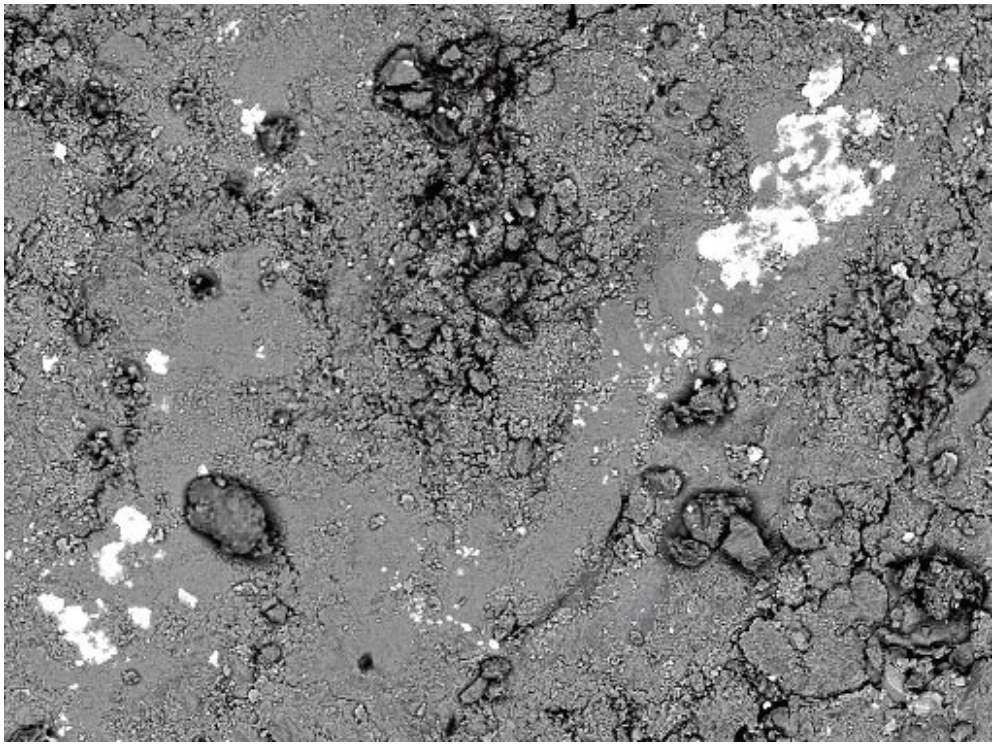

Back-scattered SEM-image of mixed layer-clay (grey) and hematite (bright crystals). Width of view is about 600 µm. Sample KLX06: 388.27–388.30 m.

Appendix 2

XRD and ICP-AES/QMS results for samples from drill cores KLX03, KLX04 and KLX06

In this section the results from XRD and ICP-AES/QMS analyses of fracture fillings/coatings are presented. The analyses were carried out by SGU (XRD) and Analytica AB (ICP-AES/QMS).

Borehole		**KLX03**	**KLX03**	**KLX03**	**KLX03**	**KLX03**	**KLX03**
Length (m)		**168.47–168.54**	**195.36–195.36**	**326.94–327.04**	**397.79–397.89**	**409.83–410.13**	**534.25–534.40**
Minerals (XRD)		**cc, qz, chl, ill, mlc**	**qz, kfs, ab, am, chl, cc, mlc**	**cc, pl, qz, chl, mlc**	**cc, qz, kfs, chl, mlc**	**qz, pl, kfs, cc, chl, mi, mlc**	**Not analysed**
SiO_2	%		48.3				9.57
Al_2O_3	%		12.4				2.85
CaO	%		5.98				34.1
Fe_2O_3	%		11.2				1.87
K_2O	%		1.91				0.632
MgO	%		3.29				0.649
MnO	%		0.135				0.0227
Na_2O	%		2.56				0.685
P_2O_5	%		0.652				0.163
TiO_2	%		1.38				0.238
Total	%		87.8				50.8
Ba	mg/kg		15,400				219
Be	mg/kg		4.64				< 0.7
Co	mg/kg		< 6				19.4
Cr	mg/kg		93.9				149
Cs	mg/kg		1.12				< 0.1
Cu	mg/kg		6.51				< 7
Ga	mg/kg		13.3				< 1
Hf	mg/kg		13				2.22
Mo	mg/kg		7.14				< 3
Nb	mg/kg		21.4				3.55
Ni	mg/kg		< 10				< 10
Rb	mg/kg		33.1				17.8
Sc	mg/kg		9				1.85
Sn	mg/kg		9.61				4.72
Sr	mg/kg		717				325
Ta	mg/kg		6.13				0.364
Th	mg/kg		9.13				2.26
U	mg/kg		6.11				1.1
V	mg/kg		173				33.3
W	mg/kg		24.3				0.802
Y	mg/kg		50.1				11.5
Zn	mg/kg		407				180
Zr	mg/kg		700				98.1
La	mg/kg		60.1				17
Ce	mg/kg		163				38.7
Pr	mg/kg		20.6				5.79
Nd	mg/kg		80				22.6

Sm	mg/kg	13.4	3.48
Eu	mg/kg	1.23	0.655
Gd	mg/kg	8.29	1.92
Tb	mg/kg	1.49	0.319
Dy	mg/kg	6.6	1.63
Ho	mg/kg	1.25	0.337
Er	mg/kg	3.87	0.865
Tm	mg/kg	0.573	0.178
Yb	mg/kg	3.65	0.994
Lu	mg/kg	0.506	0.109

ab=albite, am=amphibole, ba=barite, cc=calcite, chl=chlorite, cor=corrensite, ep=epidote, fl=fluorite, hm=hematite, ill=illite, kfs=K-feldspar, mi= mica, mlc=Mixed layer clay, mus=muscovite, qz=quartz.

Borehole		**KLX03**	**KLX03**	**KLX03**	**KLX04**	**KLX04**	**KLX04**
Length (m)		**662.33–662.65**	**743.98–744.06**	**904.38–904.54**	**193.74–193.90**	**216.66–216.79**	**352.69–352.81**
Minerals (XRD)		**cc, qz, kfs, chl, ba, mlc**	**cc, chl, kfs, cor, mlc**	**qz, kfs, chl, cc, mlc**	**qz, kfs, pl, chl, mlc**	**cc, qz, kfs, pl, chl, ill, mlc**	**cc, qz, kfs, pl, chl, ill, mlc**
SiO_2	%				62.1		
Al_2O_3	%				17.4		
CaO	%				2.6		
Fe_2O_3	%				4.25		
K_2O	%				8.15		
MgO	%				2.21		
MnO	%				0.108		
Na_2O	%				0.254		
P_2O_5	%				0.0775		
TiO_2	%				0.228		
Total	%				97.4		
Ba	mg/kg				1,020		
Be	mg/kg				13		
Co	mg/kg				< 6		
Cr	mg/kg				36.2		
Cs	mg/kg				35.8		
Cu	mg/kg				9.98		
Ga	mg/kg				32.9		
Hf	mg/kg				2.12		
Mo	mg/kg				< 2		
Nb	mg/kg				3.92		
Ni	mg/kg				< 10		
Rb	mg/kg				231		
Sc	mg/kg				2.35		
Sn	mg/kg				5.73		
Sr	mg/kg				899		
Ta	mg/kg				0.456		
Th	mg/kg				3.6		
U	mg/kg				2.56		
V	mg/kg				96.9		
W	mg/kg				0.96		

Y	mg/kg	10.6
Zn	mg/kg	218
Zr	mg/kg	84.7
La	mg/kg	50.3
Ce	mg/kg	78.6
Pr	mg/kg	8.83
Nd	mg/kg	31.8
Sm	mg/kg	3.48
Eu	mg/kg	0.658
Gd	mg/kg	1.55
Tb	mg/kg	0.314
Dy	mg/kg	1.54
Ho	mg/kg	0.251
Er	mg/kg	0.786
Tm	mg/kg	0.125
Yb	mg/kg	0.769
Lu	mg/kg	0.181

ab=albite, am=amphibole, ba=barite, cc=calcite, chl=chlorite, cor=corrensite, ep=epidote, fl=fluorite, hm=hematite, ill=illite, kfs=K-feldspar, mi= mica, mlc=Mixed layer clay, mus=muscovite, qz=quartz.

Borehole		**KLX04**	**KLX06**	**KLX06**	**KLX06**
Length (m)		**513.53–513.70**	**214.11–214.16**	**383.93–383.93**	**388.27–388.30**
Minerals (XRD)		**Not analysed**	**fl, qz, kfs, ab, chl, mlc**	**qz, kfs, ab, chl, ep, hm**	**qz, kfs, mus, chl, (ep), mlc**
SiO_2	%	21.5	40.4	43.8	53.8
Al_2O_3	%	5.08	10.5	19.5	23.8
CaO	%	32.1	25.1	5.83	1.64
Fe_2O_3	%	5.53	3.45	13.7	3.5
K_2O	%	1.68	6.83	5.39	6.86
MgO	%	3.11	1.22	4.01	4.94
MnO	%	0.184	0.0537	0.225	0.0747
Na_2O	%	0.385	0.595	0.228	0.3
P_2O_5	%	0.0595	0.037	0.482	0.195
TiO_2	%	0.131	0.0948	1.37	0.511
Total	%	69.8	88.3	94.5	95.6
Ba	mg/kg	219	2,330	550	422
Be	mg/kg	3.76	4.87	237	13
Co	mg/kg	6.6	< 6	11.4	7.94
Cr	mg/kg	64	12	118	31.8
Cs	mg/kg	1.03	8.34	103	62.3
Cu	mg/kg	25.9	7.19	27.2	21.1
Ga	mg/kg	14.1	5.63	34.9	23.6
Hf	mg/kg	7.84	8.94	6.21	4.9
Mo	mg/kg	< 2	< 2	< 2	< 2
Nb	mg/kg	2.01	2.38	15.4	9.25
Ni	mg/kg	15.4	< 10	25.3	21.2
Rb	mg/kg	34.8	119	415	348
Sc	mg/kg	8.06	4.74	20.3	3.12
Sn	mg/kg	1.64	6.46	14.4	4.12

Sr	mg/kg	86.4	54.1	1,870	402
Ta	mg/kg	0.327	1.28	1.32	0.996
Th	mg/kg	2.4	4.29	10	19.7
U	mg/kg	3.38	7.95	16.4	6.33
V	mg/kg	64.4	104	114	72.9
W	mg/kg	1.38	5.78	18.5	5.61
Y	mg/kg	48.4	93.3	36.2	13.2
Zn	mg/kg	240	312	552	267
Zr	mg/kg	22.8	32.5	323	235
La	mg/kg	47.8	73.1	99.3	11
Ce	mg/kg	57.9	77.3	168	21.7
Pr	mg/kg	10.7	7.12	22.1	2.94
Nd	mg/kg	26.4	26.4	81.8	10.7
Sm	mg/kg	5.81	4.33	11.8	2.43
Eu	mg/kg	0.947	0.885	2.66	0.546
Gd	mg/kg	5.25	4.23	8.47	1.58
Tb	mg/kg	0.456	0.828	1.27	0.335
Dy	mg/kg	3.5	5.28	5.76	1.74
Ho	mg/kg	0.913	1.13	0.973	0.423
Er	mg/kg	2.4	3.13	3.18	1.07
Tm	mg/kg	0.512	0.415	0.453	0.177
Yb	mg/kg	1.76	2.09	2.65	1.05
Lu	mg/kg	0.286	0.261	0.384	0.313

ab=albite, am=amphibole, ba=barite, cc=calcite, chl=chlorite, cor=corrensite, ep=epidote, fl=fluorite, hm=hematite, ill=illite, kfs=K-feldspar, mi= mica, mlc=Mixed layer clay, mus=muscovite, qz=quartz.

Appendix 3

$\delta^{13}C$ and $\delta^{18}O$ analyses (calcite) for samples from drill cores KLX03 and KLX04

Sample (KLX03)	$\delta^{13}C$	$\delta^{18}O$	Crystal shape
129.37–129.37	–26.4	–7.4	Equant-Scalenohedral
130.60–130.61	–3.9	–19.4	
165.52–165.55	–5.8	–11.1	
204.30–204.36A	–13.7	–7.9	Scalenohedral (short prisms)
204.30–204.36B	–10.5	–8.6	Scalenohedral (long prisms)
276.71–276.81 (1)	–6.8	–8.3	Needle
276.71–276.81 (2)	–6.5	–10.8	
288.72–288.76	–13.7	–7.9	Equant
303.21–303.21	–6.4	–9.8	
305.94–306.04	–5.3	–12.3	
327.40–327.62	–4.6	–10.6	
353.54–353.62	–15.7	–6.3	
409.83–410.13 (1)	–36.1	–7.05	Scalenohedral
409.83–410.13 (2)	–41.6	–6.8	Scalenohedral
457.33–457.42	–45.6	–7.6	Scalenohedral
590.79–590.96	–30.3	–7.4	
662.33–662.65 (1)	–5.1	–7.8	Scalenohedral
662.33–662.65 (2)	–5.7	–9.2	
771.95–772.06	–9.1	–7.9	Scalenohedral
772.24–772.27	–21	–8.1	Scalenohedral
784.71–784.79	–6.8	–10.3	
904.90–905.06	–6.1	–11.32	

Sample (KLX04)	$\delta^{13}C$	$\delta^{18}O$	Crystal shape
105.86–105.96	–7.37	–8.55	Needle
107.08–107.43 (A)	–10.1	–11.1	
107.08–107.43 (B)	–8.2	–8.5	Short c-axis
139.08–139.13	–11.3	–7.89	Needle
201.04–201.20	–9.723	–7.74	
352.69–352.81	–15.4	–6.7	Scalenohedral
513.53–513.70	–22.1	–6.2	Equant
555.27–555.44	–65.7	–7.5	Scalenohedral
580.70–580.82	–19.9	–7.9	Equant
626.51–626.58	–21.6	–8.7	Equant-short c-axis
643.18–643.40	–15	–8.6	
917.40–917.51 (1)	–13.5	–9.4	Short c-axis
917.40–917.51 (2)	–8.7	–9.4	Equant (round)
972.13–972.20	–7.18	–8.62	

Appendix 4

U-series analyses for samples from drill cores KLX03, KLX04 and KLX06

Sample	^{238}U	Error 1σ	^{235}U	Error 1σ	^{234}U	Error 1σ	^{230}Th	Error 1σ	^{232}Th	Error 1σ	$^{234}U/^{238}U$	Error 1σ	$^{230}Th/^{234}U$	Error 1σ
KLX03:168.47–168.54	40	1.3	n.a.	–	53	1.4	52	1.7	21	0.9	1.33	0.05	1	0.043
KLX03:195.36–195.36	80	1.4	n.a.	–	86	1.4	92	2.7	56	1.8	1.07	0.024	1.07	0.035
KLX03:326.94–327.04	30	2	2.24	0.58	20	2	54	3	41	2	0.69	0.08	2.67	0.26
KLX03:397.79–397.89	19	1	0.96	0.19	18	1	18	1	8	1	0.91	0.06	1.03	0.06
KLX03:409.83–410.13	42	1	1.06	0.23	36	1	41	1	55	2	0.85	0.04	1.14	0.06
KLX03:743.98–744.06	43	2	2.04	0.53	33	2	43	2	13	1	0.77	0.07	1.30	0.11
KLX03:904.38–904.54	48	1	2.17	0.21	44	1	43	2	275	7	0.90	0.03	0.99	0.06
KLX04:139.08–139.13	113	3	5.4	0.6	102	2	111	3	55	2	0.90	0.03	1.08	0.04
KLX04:193.74–193.90	35	1	1.4	0.3	41	2	42	2	30	1	1.18	0.06	1.03	0.06
KLX04:216.66–216.79	56	2	2.3	0.4	70	2	80	3	20	1	1.25	0.06	1.14	0.05
KLX04:352.69–352.81	133	3	5.4	0.5	119	2	120	3	53	2	0.89	0.03	1.01	0.04
KLX04:513.53–513.70	54	2	3	0.6	161	4	123	5	14	1	3.01	0.15	0.76	0.03
KLX06:214.11–214.16	109	1	n.a.	–	152	1	176	4	10.9	0.5	1.39	0.02	1.16	0.03
KLX06:383.93–383.93–1	212	2	n.a.	–	228	2	280	38	66.1	16	1.07	0.01	1.23	0.17
KLX06:383.93–383.93–2	214	2	n.a.	–	230	2	251	13	81	6	1.08	0.08	1.09	0.06
KLX06:388.27–388.30	56.5	3	n.a.	–	49.4	3	58.8	3	106.8	4	0.88	0.06	1.19	0.08

n.a.=not analysed

Units: Bq kg^{-1} (except for ratios).

Appendix 5

ICP-AES/QMS results for samples from KSH01A+B, KSH02 and KSH03A

		KSH01B 3.7–3.87 m	KSH01B 67.8–67.9 m	KSH01B 82.20 m	KSH01A 159.2–159.3 m	KSH01A 250.40–250.45 m	KSH01A 255.78–255.93 m
SiO_2	%	24.57	47.86	49.15	40.60	46.58	43.16
Al_2O_3	%	7.29	14.19	16.79	11.50	14.58	15.49
CaO	%	19.02	6.67	3.24	8.73	4.18	3.78
Fe_2O_3	%	11.35	8.48	11.32	14.72	10.85	10.64
K_2O	%	0.73	3.82	5.69	1.79	4.48	4.36
MgO	%	11.72	4.48	4.68	4.86	8.62	11.28
MnO	%	0.48	0.18	0.19	0.19	0.25	0.22
Na_2O	%	0.19	2.84	1.82	1.62	0.25	0.65
P_2O_5	%	< 0.01	0.33	0.42	0.34	0.23	0.43
TiO_2	%	0.05	1.35	1.07	0.99	1.31	1.61
Ba	mg/kg	165	598	1,290	9,720	1,210	964
Be	mg/kg	7.8	4.5	7.54	3.04	4.35	5.55
Co	mg/kg	14.8	16.4	24.7	< 6	21.7	23.8
Cr	mg/kg	< 10	116	78.4	144	94.2	67.9
Cs	mg/kg	3.37	9.2	36.9	1.62	2.23	2.86
Cu	mg/kg	390	41.5	190	43.7	387	351
Ga	mg/kg	17	17.3	31.1	15.8	18	23.9
Hf	mg/kg	0.439	8.63	5.88	5.82	5.3	8.37
Mo	mg/kg	< 3	< 4	< 2	17.7	9.32	< 2
Nb	mg/kg	1.19	16.3	21.2	16	13	27.3
Ni	mg/kg	13.7	28.6	28.6	< 10	22.5	26.2
Rb	mg/kg	23	121	201	42.8	108	90.1
Sc	mg/kg	10.4	23.6	51.3	21.7	20.4	27.8
Sn	mg/kg	10.8	3.74	18.9	9.52	21.8	17.5
Sr	mg/kg	132	190	198	259	461	153
Ta	mg/kg	0.184	1.19	2.93	1.29	0.96	2.22
Th	mg/kg	0.255	5.88	12.1	7.47	4.95	7.93
U	mg/kg	2.33	4.86	22.7	9.46	9.56	19.7
V	mg/kg	111	183	359	163	183	261
W	mg/kg	2.49	5.49	16.9	2.75	38.3	3.48
Y	mg/kg	74	38.9	58.4	39.4	37.3	57.2
Zn	mg/kg	356	168	313	133	360	485
Zr	mg/kg	6.18	310	241	232	234	339
La	mg/kg	67.4	59.2	673	92.2	43.7	107
Ce	mg/kg	131	114	926	170	93.7	227
Pr	mg/kg	15.6	13.4	98.8	19.6	11.4	24.8
Nd	mg/kg	67.3	58.3	387	71.9	43.8	98.3
Sm	mg/kg	13.5	10.1	35.5	11.7	7.87	14
Eu	mg/kg	3.37	2.48	5.82	1.72	2.18	3.92
Gd	mg/kg	16.9	8.6	26.9	8.68	9.42	12.9
Tb	mg/kg	2.4	1.21	3.16	1.43	1.22	1.92
Dy	mg/kg	11.9	7.54	9.59	6.91	7.02	10
Ho	mg/kg	2.33	1.47	1.92	1.42	1.37	1.91
Er	mg/kg	5.39	4.52	4.61	3.7	3.7	5.51
Tm	mg/kg	0.749	0.722	0.644	0.618	0.701	0.934
Yb	mg/kg	4.68	3.83	4.19	3.91	4	6.03
Lu	mg/kg	0.637	0.699	0.587	0.623	0.523	0.818

		KSH01A 558.60–558.65 m	KSH01A 590.36–590.52 m	KSH01A 558.60–558.65 m	KSH02 578.00–578.05 m	KSH02 743.00–743.05 m	KSH03A 272.00–272.50 m
SiO_2	%	44.02	26.28	44.02	39.3	48.5	54.8
Al_2O_3	%	14.07	9.88	14.07	15.8	15.9	16.2
CaO	%	2.20	18.32	2.20	2.9	1.73	0.962
Fe_2O_3	%	11.41	9.16	11.41	14.4	10.5	11
K_2O	%	3.40	1.12	3.40	2.62	3.64	5.22
MgO	%	12.27	12.54	12.27	12.9	10.2	4.3
MnO	%	0.33	0.46	0.33	0.339	0.233	0.097
Na_2O	%	1.54	0.60	1.54	0.966	2.9	1.23
P_2O_5	%	0.14	0.08	0.14	0.417	0.227	0.538
TiO_2	%	0.78	0.22	0.78	1.51	0.737	1.38
Ba	mg/kg	840	518	840	511	621	906
Be	mg/kg	5.05	3.98	5.05	9.8	6.09	7.56
Co	mg/kg	19.9	14.4	19.9	19.9	21.7	16.9
Cr	mg/kg	22.7	41.9	22.7	77.7	73.1	67.3
Cs	mg/kg	2.82	0.378	2.82	5.87	1.17	19.3
Cu	mg/kg	504	121	504	930	19	270
Ga	mg/kg	17.1	20.2	17.1	98.9	31.7	83.5
Hf	mg/kg	2.84	1.27	2.84	11.9	4.08	10.8
Mo	mg/kg	< 4	< 2	< 4	< 2	< 2	< 2
Nb	mg/kg	11.7	3.08	11.7	24.3	10.8	28.3
Ni	mg/kg	< 20	22.7	< 20	32.7	27.7	35.4
Rb	mg/kg	98.2	27.1	98.2	87.6	87.8	326
Sc	mg/kg	27.6	5	27.6	25.9	20.2	14
Sn	mg/kg	3.16	< 1	3.16	41.7	2.54	12
Sr	mg/kg	229	165	229	186	355	87.8
Ta	mg/kg	1.04	0.179	1.04	1.88	0.596	2.63
Th	mg/kg	3.82	1.45	3.82	13.8	8.31	15.8
U	mg/kg	9.77	0.909	9.77	8.31	6.98	23.2
V	mg/kg	253	147	253	122	114	94.8
W	mg/kg	1.89	0.953	1.89	8.64	7.41	7.75
Y	mg/kg	35.9	6.2	35.9	64.6	33.4	36.1
Zn	mg/kg	523	384	523	1,130	470	236
Zr	mg/kg	118	52.3	118	487	166	504
La	mg/kg	44.6	13.4	44.6	71.3	55.7	25.6
Ce	mg/kg	86.9	21.5	86.9	157	107	48
Pr	mg/kg	9.69	2.2	9.69	21.9	12.8	8.83
Nd	mg/kg	33.1	9.81	33.1	77.4	46	24.9
Sm	mg/kg	6.81	1.31	6.81	13.9	8.36	4.69
Eu	mg/kg	1.8	0.367	1.8	3.18	1.63	1.07
Gd	mg/kg	8.13	1.57	8.13	9.17	6.82	3.22
Tb	mg/kg	1.37	0.168	1.37	1.01	1.01	< 0.1
Dy	mg/kg	6.36	0.926	6.36	11.9	5.33	5.78
Ho	mg/kg	1.25	0.183	1.25	2.26	1.06	1.25
Er	mg/kg	3.6	0.743	3.6	6.26	2.82	4.04
Tm	mg/kg	0.657	0.159	0.657	0.971	0.493	0.73
Yb	mg/kg	4.42	0.674	4.42	7.03	3.07	4.56
Lu	mg/kg	0.642	0.118	0.642	0.974	0.399	0.768

Appendix 6

U-series analyses for samples from KSH01A+B, KSH02 and KSH03A

Sample	^{238}U	Error 1σ	^{235}U	Error 1σ	^{234}U	Error 1σ	^{230}Th	Error 1σ	^{232}Th	Error 1σ	$^{234}U/^{238}U$	Error 1σ	$^{230}Th/^{234}U$	Error 1σ
KSH01B: 3.70–3.87 m	48.2	1	n.a.	–	65.7	1.2	41.6	1.6	2.3	0.3	1.36	0.05	0.63	0.04
KSH01B: 8.6 m	55.4	1.7	n.a.	–	58.1	1.7	65.2	2.3	26.3	1.3	1.05	0.06	1.12	0.07
KSH01B: 8.70–8.75 m	174	6	n.a.	–	194	6	265	8	117	5	1.11	0.08	1.37	0.09
KSH01B: 67.8–67.9 m	49.9	1.4	n.a.	–	50.1	1.4	63.2	2.6	50.3	2.2	1.00	0.06	1.26	0.09
KSH01B: 82.2 m	356	11	n.a.	–	381	11	283	23	53.7	5.6	1.07	0.07	0.74	0.08
KSH01A: 159.2–159.3 m	136	2	n.a.	–	134	2	102	2	34.9	0.9	0.99	0.03	0.76	0.03
KSH01A: 250.40–250.45 m	178	3	n.a.	–	191	3	176	4	41	1.3	1.07	0.04	0.92	0.04
KSH01A: 255.78–255.93 m	305	7	n.a.	–	327	8	285	16	49	3.9	1.07	0.05	0.87	0.07
KSH01A: 558.60 m	187	4	n.a.	–	210	5	209	5	33	1.4	1.12	0.05	1.00	0.05
KSH01A: 590.36–590.52 m	12.5	0.4	n.a.	–	12	0.4	14.2	0.6	8.3	0.4	0.96	0.06	1.18	0.09
KSH02: 289.00–289.05 m	144	1	5.1	0.17	148	1	170	6.1	38	2.4	1.03	0.01	1.15	0.04
KSH02: 578.00–578.05 m	96	0.78	3.7	0.15	94.4	0.77	112	4.1	72	3.1	0.98	0.01	1.19	0.05
KSH03A: 272.00–272.50 m	301	2.6	10.6	0.47	336	2.78	377	7.4	103	2.9	1.12	0.01	1.12	0.02

Units: Bq kg^{-1} (except for ratios)
n.a. = not analysed

Appendix 7

XRD analyses for samples from KSH02

KSH02: 289.00–289.05 m

Whole rock (WR)

The sample mainly consists of quartz, calcite, plagioclase, K-feldspar, chlorite and hematite.

Fine fraction

The fine-grained material is mostly chlorite but a mixed-layer clay mineral of corrensite-type (not well structured layers) and some hematite is also present.

KSH02: 578.00–578.05 m

Whole rock (WR)

Chlorite is the dominating mineral. Other minerals are quartz, K-feldspar, plagioclase, small amounts of hematite and probably also talc.

Fine fraction

The fine fraction is dominated by chlorite. Other minerals are a mixed-layer clay mineral of corrensite-type (not well structured layers, similar as KSH02: 289 m) and small amounts of K-feldspar, hematite and probably also talc.

KSH02: 743.00–743.05 m

Whole rock (WR)

Identified minerals are: Quartz, plagioclase, K-feldspar, hematite and chlorite.

Fine fraction

The fine fraction is dominated mixed-layer clay of corrensite-type. Other minerals are chlorite and small amounts of hematite.

Appendix 8

$\delta^{13}C$ and $\delta^{18}O$ analyses (calcite) from KSH02

Sample name (KSH02)	$\delta^{13}C$	$\delta^{18}O$
104.00 (subsample 1)	–13.24	–8.63
104.00 (subsample 2)	–14	–8.37
422.90	–12.3	–6.63
423.00	–10.26	–6.78
743.00–743.05	–7	–11.54